Study of Neuropathogenesis in Myotonic Dystrophy type 1 in *Drosophila* Model Organism

DISSERTATION REPORT SUBMITTED TO

NATIONAL BRAIN RESEARCH CENTRE

(DEEMED TO BE UNIVERSITY)

For the partial fulfilment of

MASTER OF SCIENCE (M.Sc.) NEUROSCIENCE

Submitted By

RITU SARKAR

BATCH 2023-2025

UNDER THE SUPERVISION OF

Dr. M. DHRUBA SINGH

NATIONAL BRAIN RESEARCH CENTRE

(DEEMED UNIVERSITY)

MANESAR, GURUGRAM – 122052

ब्रिक – राष्ट्रीय मस्तिष्क अनुसंधान केंद्र
BRIC – National Brain Research Centre
(जैव प्रौद्योगिकी अनुसंधान एव नवाचार परिषद, भारत सरकार)
एन० एच०–08, मानेसर–122 052 (हरियाणा), भारत
(An Institute of the Biotechnology Research and Innovation Council, Govt. of India)
NH-08, Manesar - 122 052 (Haryana), INDIA

CERTIFICATE

This is to certify that the dissertation report entitled '**Study of Neuropathogenesis in Myotonic Dystrophy type 1 in *Drosophila* Model Organism**' is the result of work carried out by **Ms. Ritu Sarkar** in the Division of Cellular and Molecular Neuroscience, National Brain Research Centre, Manesar, Haryana, India, for partial fulfillment of requirements for the M.Sc. degree.

The work presented herein is original and has not been submitted previously for the award of any degree or diploma to the **National Brain Research Centre (Deemed to be University)** or any other University. This work is based on the guidelines of the **National Brain Research Centre (Deemed to be University)** and is a record of the candidate's own efforts.

Dr. M. Dhruba Singh
(Supervisor)

(Director, NBRC)

Place: Manesar
Date: 20.06.2025

डा. मायांगलमबम धूबा सिंह
Dr. Mayanglambam Dhruba Singh
वैज्ञानिक IV / Scientist IV
राष्ट्रीय मस्तिष्क अनुसंधान केन्द्र
National Brain Research Centre
मानेसर, गुड़गाँव- 122052 (हरियाणा)
Manesar, Gurgaon-122052 (Haryana)

DECLARATION BY CANDIDATE

I, **Ritu Sarkar**, hereby declare that the work presented in the dissertation report entitled **'Study of Neuropathogenesis in Myotonic Dystrophy type 1 in *Drosophila* Model Organism'** was carried out by me under the guidance of **Dr. M Dhruba Singh,** Division of Cellular and Molecular Neuroscience, **National Brain Research Centre (Deemed to be University)**, Manesar, Haryana, India.

I declare that no part of the thesis contains any plagiarized material, and any previously published or other material sourced from anywhere else has been appropriately attributed to the source.

I also declare that no part of this thesis has been previously submitted for the award or any degree or diploma to the **National Brain Research Centre (Deemed to be University)** or to any other university.

Place: Manesar

Ritu Sarkar

Date: 23rd June, 2025

Acknowledgment

I would like to express my gratitude to my supervisor, Dr. M. Dhruba Singh, for granting me the opportunity to work under his guidance and entrusting me with a project to lead. Under his supervision, I have learned to develop scientific thinking, honed my ability to communicate research effectively, and gained a deeper understanding of the nuance of scientific inquiry. I appreciate his insightful feedback, constructive suggestions, and unwavering support throughout my research journey. His method of approach to problem-solving and dedication to excellence have greatly influenced my growth as a researcher.

I extend my heartfelt thanks to my lab-seniors and lab mates, Dr. Naorem Tarundas Singh, Ms. Dipti Chakraborty, Ms. Athira M. Sarath, Ms. Deepti Thapliyal, and Ms. Shreya Borthakur, for their invaluable mentorship, camaraderie, and support. They created a great work environment in which to thrive. A special thank you to our lab technicians, Mr. Mithlesh K. Singh and Mr. Hari Shankar, for their meticulous management of the indents and paperwork, for keeping the flies fed, and for ensuring the smooth operation of our research. Also, thanks to the rest of the lab, Mr. Saurabh Bajpayee, and Ms. Bhawna, for keeping the lab environment vibrant and uplifting.

Thanks to my family —my parents and my sister — for their unwavering support throughout my journey. To Ms. Gauri Shintre and Mr. Maulik Patel, for sharing my joys, stresses, all the late-night walks and conversations that kept me grounded. All the batchmates, NBRC seniors and juniors, for keeping NBRC lively and happening, helping me make some great memories, and sharing a laugh with me.

Abbreviations

ANOVA: Analysis of Variance

Atg: Autophagy-related Gene

CCA: Cardiac conduction abnormalities

CNBP: Cellular Nucleic Acid-Binding Protein

CNS: Central Nervous System

CRA: Cardiac Rhythm Abnormalities

CTG: Cytosine-Thymine-Guanine

CUGBP1: CUG-binding protein 1

DANs: Dopaminergic Neurons

DM: Myotonic Dystrophy

DM1: Myotonic Dystrophy Type 1

DMPK: Myotonic Dystrophy Protein Kinase

IF: Immunofluorescence

MB: Mushroom body

MBNL1: Muscleblind-like 1

Nt: Nucleotide

OANs: Octopaminergic Neurons

PAL: Posterior Antennal Lobe

PAM: Protocerebral Anterior Medial

PKC: Protein Kinase C

PNs: Projection Neurons

PPL1/2: Protocerebral Posterior Lateral 1/2

PPM1/2: Protocerebral Posterior Medial1/2

PPM3: Protocerebral Posterior Medial 3

Ref(2)P: Refractory to Sigma P

RNA: Ribonucleic Acid

siRNA: small interfering RNAs

T1: Thoracic 1

UAS: Upstream Activating Sequence

UTR: Untranslated Region

VUM: Ventral Unpaired Median

WB: Western Blot

List of Figures

Figure 1: Genetic background of Myotonic dystrophy type 1 and type 2

Figure 2: Pathological process behind DM1 according to RNA gain-of-function hypothesis.

Figure 3: Graphic representation of the UAS/Gal4 system.

Figure 4: Graphic representation of UAS/Gal4 with Gene-Switch System.

Figure 5: Expression of CTG270 in neuronal tissues causes reduced longevity.

Figure 6: Validation of the Elav-GS Gal4

Figure 7: Quantification of γ lobe degeneration at 10 days and 25 days.

Figure 8: Expression of expanded CUG repeats in dopaminergic neurons results in degeneration and reduction in the DANs cluster.

Figure 9: RNA foci are formed in the adult brain.

Figure 10: Upregulation of autophagy in the CTG270 expressing fly brain.

Contents

1. Introduction …….....10-18

1.1. What is DM1?

1.1.1. Factors Affecting the Genetics of DM1

1.1.2. Mechanism of DM1 Pathogenesis

1.1.3. Clinical Manifestation of DM1

1.1.4. Why do we study DM1 in brain?

1.2. Drosophila Model System

1.2.1. Life Cycle of *Drosophila*

1.2.2. Balancers and Markers

1.2.3. UAS and GAL4 System

1.2.4. GAL4 Driver with Gene-Switch

1.3. Structures of Drosophila

1.3.1. Mushroom Body

1.3.2. Dopaminergic Neurons (DANs)

2. Aim and Objectives…….....19

3. Result……..…..20-29

3.1. Effects of DM1 on Behaviour and Neurodegeneration in *Drosophila melanogaster*

3.1.1. Selection Of Gal4 Lines and Survival Analysis

3.1.2. CUG-Expanded Repeats Cause Degeneration of the γ Lobe of The Mushroom Body

3.1.3. Effects Of CUG Repeats on The Dopaminergic Clusters Present In *Drosophila*

3.1.4. Increased CUG Repeats Lead to Toxic RNA-Foci Formation

3.2. Investigation of the Autophagic Pathway in DM1 Drosophila brain

3.2.1. The expression of autophagy-related genes in adult brain in DM1 flies

4. Discussion…….30-32

4.1. CTG Repeat Expression in Neuronal Tissues Reduces Longevity and Induces Neurotoxicity

4.2. Mushroom Body Degeneration Suggests Targeted Neuronal Vulnerability

4.3. Dopaminergic Neuron Loss and Locomotor Deficits Recapitulate Motor Symptoms

4.4. RNA Foci Formation Confirms Molecular Signature of DM1

4.5.Dysregulation of Autophagy Highlights a Key Mechanism of Neuronal Dysfunction

4.6. Limitations and Future Directions

5. Materials and Methods……...33-43

6. References…….…..44-50

1. Introduction

Myotonic dystrophy (DM) is a genetically inherited disorder characterized by progressive muscle wasting and neurodegeneration. The term 'myotonic' came from the word 'myotonia', defined as the impaired relaxation of muscles following contraction. DM is classified into two types.

Myotonic dystrophy type 1 (DM1), also known as Steinert disease (OMIM 160900), was first discovered by Wilhelm Steinert in 1909. It arises from an expansion of unstable CTG (cytosine-thymine-guanine) trinucleotide repeats in the 3' untranslated region (UTR) of the Myotonic Dystrophy Protein Kinase (DMPK) gene, located on chromosome 19q13.3.

Myotonic dystrophy type 2 (DM2) results from an unstable CCTG tetranucleotide repeat expansion in the Cellular Nucleic Acid-Binding Protein (CNBP) gene (previously termed Zinc Finger 9, ZF9) on chromosome 3q21.

Although DM1 and DM2 share overlapping clinical features, they exhibit notable differences, establishing them as two distinct diseases. This study focuses on DM1 and its underlying pathophysiology.

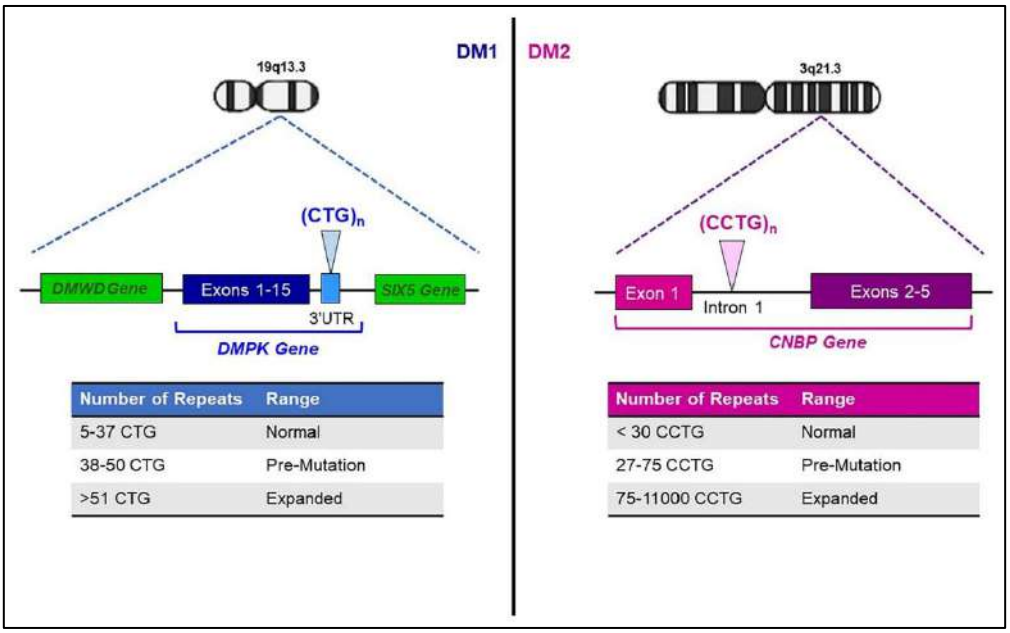

Figure 1: Genetic background of Myotonic dystrophy type 1 and type 2. DM1 is caused by $(CTG)_n$ expansion in the 3' UTR of the DMPK gene. A healthy individual contains $(CTG)_{5\text{-}37}$, whereas a diseased individual carries $(CTG)_{>51}$. DM2 manifests due to $(CCTG)_n$ repeats in the CNBP gene. Alleles with $(CCTG)_{<30}$ is considered healthy, but $(CCTG)_{75\text{-}11,000}$ leads to the disease manifestation. (Image taken from, Epigenetics of Myotonic Dystrophies: A Minireview, https://doi.org/10.3390/ijms222212594)

1.1. What is DM1?

Myotonic dystrophy type 1 (DM1) is a multi-systemic, autosomal dominant disorder and the most prevalent form of DM, with a global prevalence of 9.27 individuals per 100,000. The severity of the disease correlates with the number of CTG repeats present in the DMPK gene: 5 to 37 repeats are present in healthy individuals, whereas 50 to 150 repeats often exhibit mild symptoms, and 100 to 1000 repeats lead to severe cases of DM1.

Based on the repeat length, DM1 is categorized into five clinical subtypes [1]:

Subtypes	CTG Repeat Length	Onset
Congenital DM1	~750 –1300	Birth (neonatal)
Infantile Onset	~500 –1000	Early childhood
Juvenile Onset	~400 –750	Adolescence
Adult Onset	~350 –700	Early-to-mid adulthood
Late Onset	~50 – 600	Late adulthood

Larger CTG expansions correlate with earlier disease onset and increased severity, and an inverse correlation exists between the age of symptom manifestation and the number of repeats [42].

1.1.1. Factors Affecting the Genetics of DM1

A hallmark of DM1 is genetic anticipation. It is a phenomenon where the disease manifests at an early age and with more severe symptoms in successive generations of an affected family. This is explained by the instability of the trinucleotide expansion, along with its tendency to expand in successive generations.

The two critical factors contributing to the degree of expansion in the transmission of the mutations are:

(1) Parental repeat size: larger expansions in the transmitting parent increase the likelihood of further expansion in offspring.

(2) Sex of the transmitting parent: Previous literature suggests that intergenerational variation is higher in cases of maternal transmission than in those of paternal transmission [3,4]. It is also observed that in 91% of cases of congenital DM1, the disease is transmitted from the maternal side [7 5]. Whereas 67% of juvenile, 68% of

adult, and 63% of late-onset cases of the disease are more frequently transmitted paternally [86].

1.1.2. Mechanism of DM1 pathogenesis

- **RNA gain-of-function hypothesis:**

The unstable CTG repeats present in the DMPK gene contribute to the underlying molecular mechanism and progression of DM1 pathophysiology through toxic RNA gain-of-function and disrupted splicing regulation. The RNA gain-of-function hypothesis and aberrant sequestration of MBNL1 by the CUG repeats are the most sought-after.

The transcribed expanded CUG repeats form a hairpin structure with C-G base pairs and bulged U residues. The U residues have a high binding affinity with MBNL1 proteins. Muscleblind-like 1 (MBNL1) and CUG-binding protein 1 (CUGBP1) are two alternative splicing regulators. Due to the RNA gain-of-function, the MBNL1 protein gets sequestered with the hairpin structure, leading to the formation of ribonuclear foci (Fig. 1).

This transcribed mRNA also activates protein kinase C (PKC), which leads to hyperphosphorylation and upregulation of CUGBP1. Thus, a decrease in free MBNL1 and an increase in free CUGBP1 result in the misexpression of splicing patterns in adult tissues, leading to the manifestation of disease phenotypes [7-11].

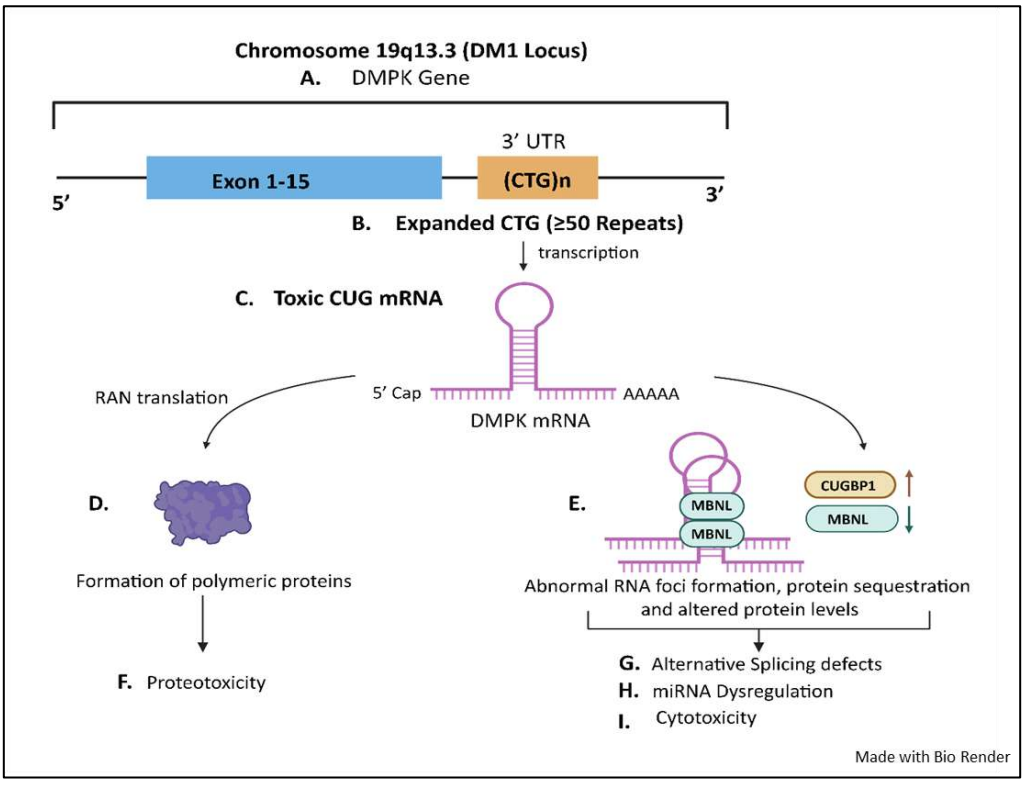

Figure 2: Pathological process behind DM1 according to RNA gain-of-function hypothesis

- **Triple repeat-derived siRNAs enhance pathogenesis:**

The DM1 gene exhibits bidirectional transcription, resulting in the formation of both anti-sense CAG repeat transcription and sense CTG repeat transcription, which are responsible for disease pathogenesis. During bidirectional transcription, these transcripts produce small interfering RNAs (siRNA). These siRNAs are capable of breaking the expanded CUG-repeats into shorter CUG-fragments of (~21 nt), which still retain MBNL1-binding ability, contributing to additional RNA foci formation [12]. These short CUG repeat fragments act as a substrate for RAN translation and produce toxic polyglutamine peptides, resulting in proteotoxicity and enhanced neurodegeneration [13].

1.1.3. Clinical Manifestation of DM1

DM1, caused by CTG repeat expansion in the DMK gene, is a multisystemic disorder affecting muscles, the central nervous system, cardiovascular system, respiratory system, endocrine system, and the eyes. Chronic fatigue, insulin resistance, and gastrointestinal dysmotility also contribute to the reduction in quality of life and daily functioning [14-16].

- **Musculoskeletal System:** Myotonia, and muscle atrophy are the initial symptoms to manifest in DM1, resulting in lower limb weakness. Gait impairments, reduced gait speed, shorter stride length, and difficulties with balance follow after [17,18].
- **Central Nervous System (CNS):** Studies have reported that patients with DM1 exhibit a significant reduction in gray matter mass, a decrease in white matter volume, and an increase in white matter lesions [19,20]. The CNS involvement leads to cognitive and neuropsychological impairments, such as apathy, emotional disengagement, attention deficit, executive dysfunction, and emotional regulation, which have been noted in individuals with DM1 [20-23].
- **Cardiovascular System:** Cardiac conduction abnormalities (CCA) and cardiac rhythm abnormalities (CRA) in DM1 constitute a significant cause of mortality. Patients often suffer from arrhythmias, heart blockages, and an increased risk of sudden cardiac death [24,25].
- **Respiratory System:** Respiratory failure is another life-threatening complication seen in DM1 patients. Progressive muscle wasting of the respiratory tract leads to impaired gas exchange functions, lung, and pump failure, restricted pulmonary function, hypoventilation, low oxygen levels in the blood, and the inability to remove carbon dioxide [26,27]. Initially, respiratory failure tends to manifest in the form of

pneumonia, asthma, or upper respiratory disorder. Patients are often observed to need mechanical ventilation [28].

- **Visual System:** Cataract development in early-onset DM1 is one of the most common manifestations observed [29-31].
- **Endocrine System:** Previous studies have recorded the progressive nature of endocrine dysfunction observed in individuals with DM1. As the disease progresses, there is an increase in hyperthyroidism, diabetes, abnormal TSH level, and androgen insufficiency [32]. Impaired glucose tolerance, abnormal glucose metabolism, and insulin resistance, which is compensated by hyperinsulinaemia, are noticed in all individuals with DM1 [33]. A high prevalence of hypogonadism and erectile dysfunction in men also contributes to the hormonal dysfunction [34].
- **Gastrointestinal System:** Both the upper and lower gastrointestinal tracts are affected in DM1; symptoms include dysphagia, heartburn, abdominal pain, constipation, bloating, diarrhea, and changes in bowel habits [35].

1.1.4. Why do we study DM1 in brain?

Traditionally classified as a muscular disorder, myotonic dystrophy type 1 (DM1) is now recognised as a multisystemic disease with significant central nervous system (CNS) involvement [19-23,36]. Emerging evidence demonstrates that neurodegenerative pathology contributes substantially to DM1 progression, warranting focused research on its neurological manifestations.

Histological studies have found the accumulation of inclusion bodies, cellular alterations in neurons, and glial alterations in the limbic system, cerebral cortex, basal ganglia, brainstem, and cerebellum [37].

DM1 patients exhibit not only CNS-driven symptoms (as mentioned in Section 1.1.3) that impair their quality of life, but also RNA-mediated defects, such as splicing misregulation, synaptic defects due to free MBNL1 loss [38], exocitotoxicity due to increased CELF1 (a member of CUGBP) [39], mitochondrial dysfunction, and Tau hyperphosphorylation, resulting in neuronal vulnerability.

There are studies suggesting neuromuscular transmission abnormalities in cohorts of DM1 patients [40,41]. The mutant mRNA aggregates are also detected in the nuclei of spinal motoneurons of DM1 patients [42].

DM1 in the brain exhibits neurofibrillary tangles due to MAPT mis-splicing, a phenomenon similar to Alzheimer's disease [43], and motor neuron degeneration similar to Amyotrophic Lateral Sclerosis (ALS).

Current treatment, therapeutics regarding DM1 include physical therapy and assistive devices for mobility and muscle functioning, speech and swallowing therapy for dysarthria and dysphagia, and sodium-channel blockers like mexiletine for myotonia. But current therapies fail to address cognitive decline, neuropsychiatric symptoms, and progressive neurodegeneration in brain degeneration. Thus, understanding brain and CNS-specific mechanisms is necessary for developing targeted neuroprotective therapies.

1.2. Drosophila Model System:

Drosophila, as a model system, is proven to be a powerful model organism for studying neurodegenerative and neurological diseases, as many genes and molecular pathways involved are conserved in flies. With the help of transgenic lines, CUG-repeat expansion has been modeled in flies, resulting in similar RNA foci formation and mis-splicing events. Muscle degeneration, synaptic defects, and behavioural changes mimic human DM1 symptoms. The short lifespan of flies (~2 months) allows for a rapid assessment of disease progression and potential therapeutic interventions**.** The UAS/Gal4 system, transgenics, and RNAi allow the easy manipulation of genes associated with DM1**.**

1.2.1. Life Cycle of *Drosophila*:

There are three stages of development in *Drosophila* before it becomes an adult fly. Embryonic development and zygote formation occur within the egg membrane. At 25°C, after 24 hours, the eggs hatch into the larval stage. Over the next five days, the larvae undergo three instar stages (first instar, second instar, and third instar) before progressing to the pupal stage. They remain in pupal form for 3.5 to 5 days before eclosing into adult form. Thus, at 25°C, the complete life cycle takes approximately 10 days, with an average adult lifespan of 70 days.

1.2.2. Balancers and Markers:

Balancer chromosomes in *Drosophila* contain multiple chromosomal inversions that suppress meiotic recombination, helping to maintain lethal and sterile mutations in a

stable population. They also carry specific markers as dominant and recessive mutation alleles. The balancer chromosomes often exhibit recessive lethal or sterile mutations, forcing a heterozygous condition in a stable population.

For example, Chromosome 3 has the balancer TM6B (Third Multiple 6B), which is lethal in a homozygous condition. The dominant marker for TM6B is tubby (Tb) (a short, stocky body phenotype) and recessive marker is ebony (e) (dark body colour).

1.2.3. UAS and GAL4 System:

The UAS/Gal4 system is a genetic tool used to control gene expression in a tissue-specific manner. GAL4 is a yeast transcriptional factor that binds to UAS (Upstream Activating Sequence). UAS is a DNA sequence that, upon binding with GAL4 protein, activates transcription of the downstream gene. Effector gene is placed under the control of UAS sequence.

In Drosophila, the GAL4 driver and the UAS responder are combined via crossing. GAL4 activates transcription of the UAS sequence, leading to expression of the effector gene only in cells where GAL4 is present.

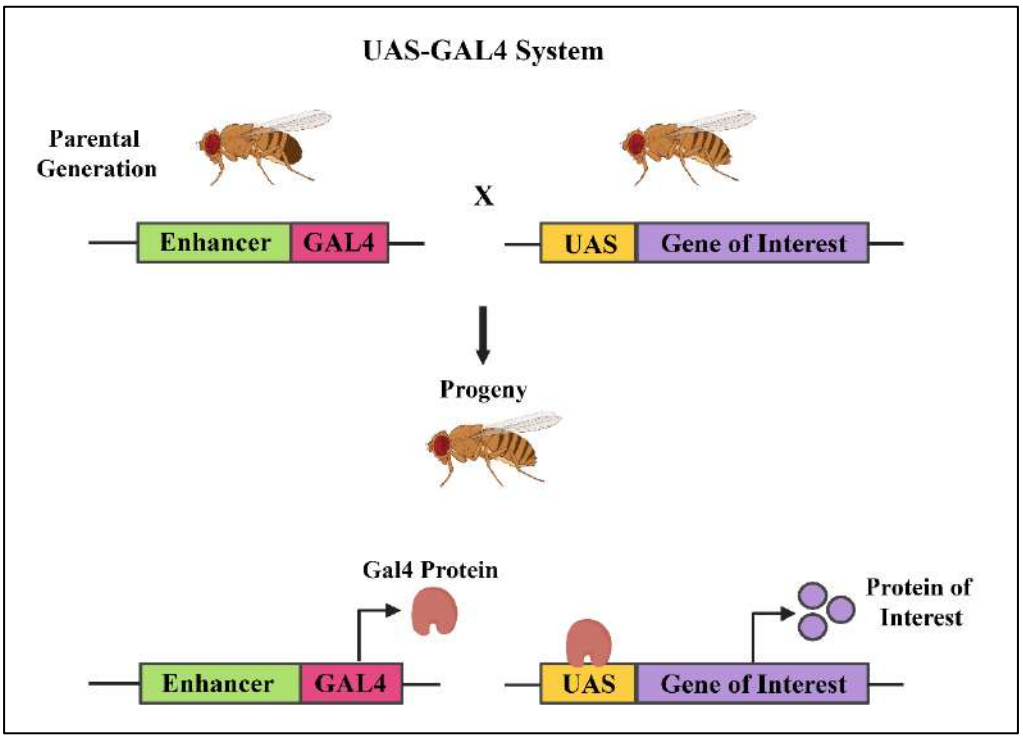

Figure 3: Graphic representation of the UAS/Gal4 system (made by using BioRender)

1.2.4. GAL4 Driver with Gene-Switch:

The Gene-Switch GAL4 system is a drug-inducible UAS/GAL4 system in the *Drosophila* model organism with a GAL4-progesterone receptor fusion protein. The UAS expression is induced by adding RU486 (mifepristone) to the fly food. GAL4 driver with Gene-Switch is helpful in studying the adult-onset of a disease's expression.

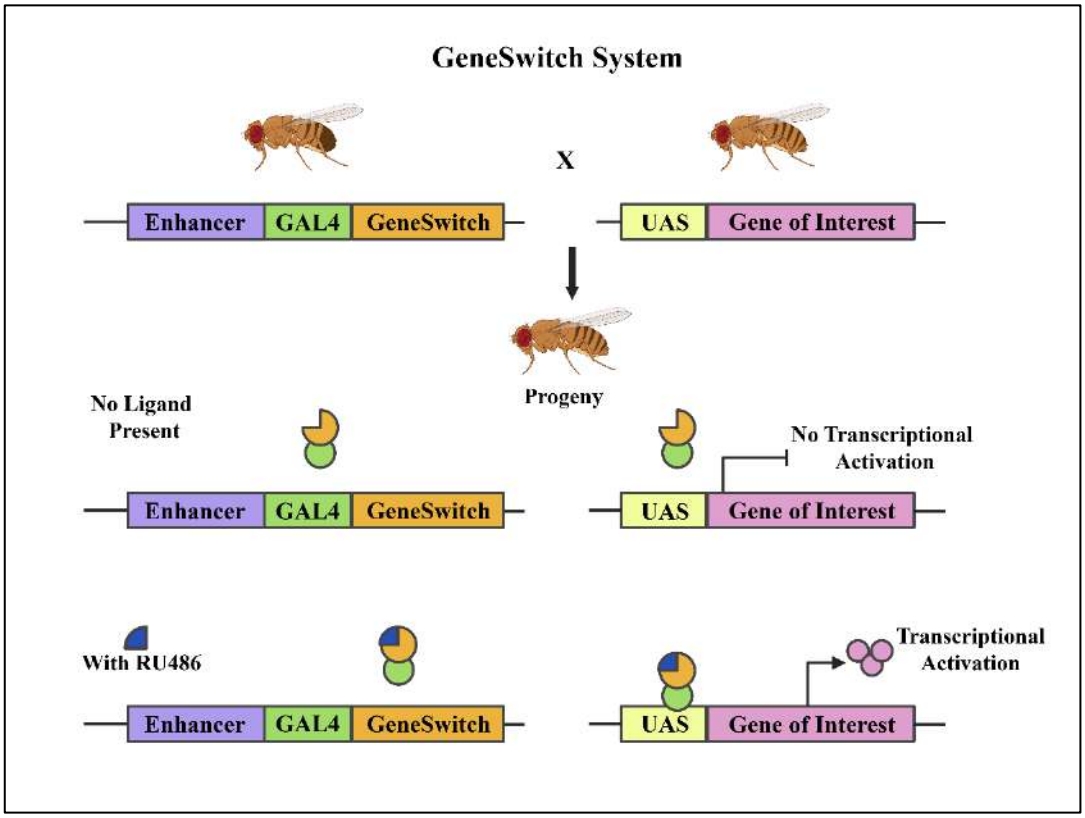

Figure 4: Graphic representation of UAS/Gal4 with Gene-Switch System (made using BioRender).

1.3. Structures of Drosophila:

1.3.1. Mushroom Body:

The Mushroom body (MB) of *Drosophila* is a neuropil, a dense network of neuronal processes, comprising Kenyon cell dendrites (which receive inputs in the calyx), Kenyon cell axons (forming the MB's lobes), and extrinsic neurons that provide modulation and output pathways. The MB is divided into three primary lobes, α, β, and γ lobes, which transmit processed signals via MBONs (MB Output Neurons). Kenyon cells act as second-order neurons, integrating sensory information relayed by projection neurons (PNs, chiefly

olfactory), modulatory inputs from dopaminergic (DANs) and octopaminergic neurons (OANs)**,** and indirect cues from visual and mechanosensory pathways. The γ lobe is particularly linked to short-term memory and olfaction, while the α/β lobes are implicated in long-term memory formation [44-46].

1.3.2. Dopaminergic Neurons (DANs):

In *Drosophila*, dopaminergic neurons are organised in distinct clusters that comprise a defined number of cells throughout the head and ventral nerve cord [47-51].

PAM (Protocerebral Anterior Medial) cluster: drives reward learning and appetitive memory via input to specific MB lobes.

PPL1/2 (Protocerebral Posterior Lateral 1): drives aversive memory, e.g., electric shock and bitter taste by targeting MB lobes.

PPM1/2 (Protocerebral Posterior Medial1/2): regulates sleep and arousal.

PPM3 (Protocerebral Posterior Medial 3): drives Aversive memory and locomotion regulation by targeting MB.

PAL (Posterior Antennal Lobe): olfaction processing, modulates antennal lobe output by targeting antennal lobe glomeruli.

T1 (Thoracic 1): helps in mechanosensation and escape behaviour by sending input to the ventral nerve cord (VNC).

VUM (Ventral Unpaired Median): helps in extension of the proboscis and initiates feeding by targeting the suboesophageal zone (SEZ).

2. Aim and Objectives

While DM1 is classically viewed as a neuromuscular disorder, its profound CNS manifestations, including cognitive decline and motor impairment, lack effective treatments. By systematically analysing neuronal RNA toxicity**,** dopaminergic degeneration, and autophagy dysregulation in a *Drosophila* DM1 model, this work provides a mechanistic foundation for CNS-specific therapeutic strategies to alleviate the disease burden.

Aim: To investigate the neurodegenerative effects of CUG repeat expansion in *Drosophila melanogaster*, modelling myotonic dystrophy type 1 (DM1), and to elucidate the role of autophagy dysregulation in disease progression.

Objectives:

I. **Effects of DM1 on Behaviour and Neurodegeneration in *Drosophila melanogaster***

- Assess the impact on lifespan and survival.
- To characterize CUG repeat-induced neuroanatomical defects.
- To correlate neuropathology with behavioural defects.
- Comprehensive study of the Autophagic Pathway in DM1 Drosophila brain

II. **Investigation of the Autophagic Pathway in DM1 Drosophila brain**

- To investigate autophagy dysregulation in DM1 brain.
- Comparing autophagy gene expression with behavioural and neuroanatomical phenotypes to identify potential therapeutic targets.

3. Results

3.1. Effects of DM1 on Behaviour and Neurodegeneration in *Drosophila melanogaster*

3.1.1. Selection Of Gal4 Lines and Survival Analysis

To model DM1 in flies, we used transgenic lines carrying 270 CTG repeats of dsRed cloned at the 3' UTR of the DMPK gene, a pathogenic repeat length associated with the adult-onset of disease phenotype. The non-pathogenic 19 CUG repeat expansion, as well as UAS-GFP and UAS-LacZ lines, were used as controls. To evaluate the brain-related phenotypes, we expressed the CTG270 in neuronal tissues using 201y-Gal4, Ple-Gal4, D42-Gal4, and Elav-GS, which express in mushroom body neurons, dopaminergic neurons, motor neurons, and the whole nervous system, respectively (Table 1, Fig. 1). The neuronal expression of abnormal CTG repeats caused a significant reduction in the longevity of the flies (Table 1, Fig. 1, $p < 0.0001$, log-rank Mantel-Cox test). The expression of CTG270 with Elav-Gal4 caused lethality at the larval stage,

whereas Elav-GS caused reduced lifespan with a mean lifespan of 6±0.16. Similarly, expression in mushroom body neurons and dopaminergic neurons caused reduced longevity (Table 1, Fig. 1). The study indicates that expression of abnormal CTG repeats could induce neurotoxicity and reduce the overall lifespan of the flies.

Table 1: Mean survival age of flies with 270 CTG expansion in tissue-specific expression:

Gal4 Line	Mean Age (in days)
Elav-Gal4 (Pan-neuronal driver)	Lethal (death at larval stage)
Elav-GS (Pan-neuronal driver)	6±0.16 (drug fed starting day 1 after eclosion)
201Y-Gal4 (Mushroom Body driver)	25±1.65
Ple-Gal4 (Dopaminergic neuron driver)	33±1.34
D42-Gal4; UAS-nSyb GFP (Motor neuron driver)	28±2

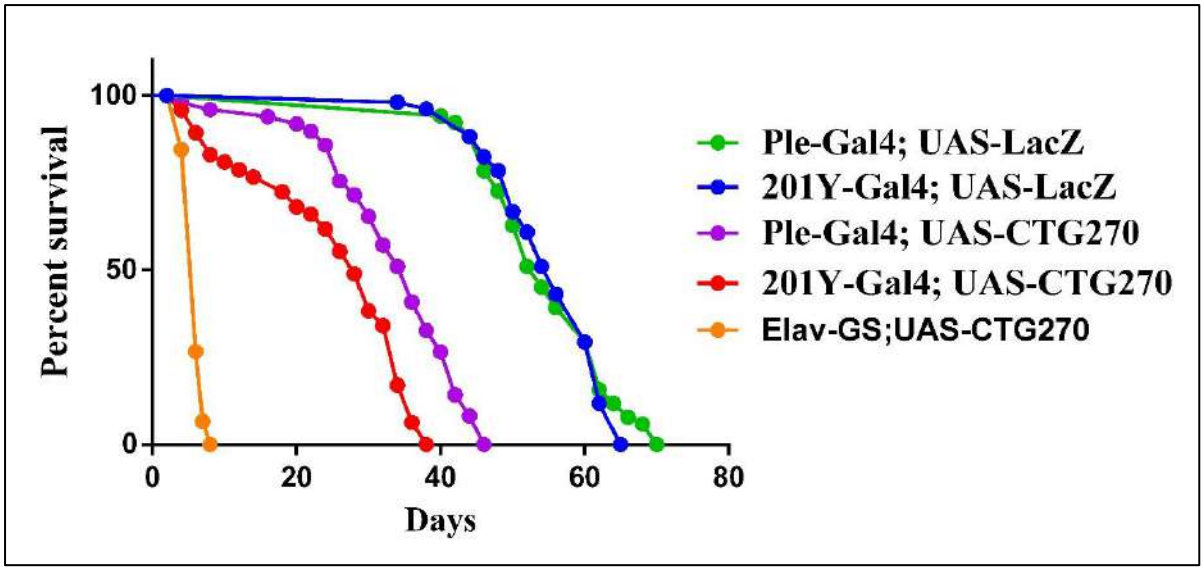

Figure 5: Expression of CTG270 in neuronal tissues causes reduced longevity: The mean lifespan of Ple-Gal4; UAS-LacZ (n=62), 201Y-Gal4; UAS-LacZ (n=55) is 50±1.6 and 55±1.07, respectively. On other hand, Ple-Gal4; UAS-CTG270 (n= 55), Elav-GS; UAS-CTG270 (n= 45). 201Y-Gal4; UAS-CTG270; (n = 53) showed a significant reduction in lifespan. The Survival curve was generated by the Kaplan-Meier method (in days) ($p < 0.0001$, Log-rank Mantel-Cox test). Mean survival has been reported as the mean ± standard error (SE).

To validate the Elav-GS line, we fed the flies with RU486 (mifepristone). First, we investigated at what dosage the RU486 induces the Elav-GS. We observed that at a concentration of 100 µg/1 ml, RU486 was able to induce GFP expression, indicating the induction of Elav-GS in comparison to flies not fed RU486 (Fig. 6A-B). Moreover, the CTG270 flies fed with RU486 exhibit reduced climbing ability at day 5 (Fig. 6C). Additionally, these flies do not survive beyond 7 days (Fig. 4, Table 1).

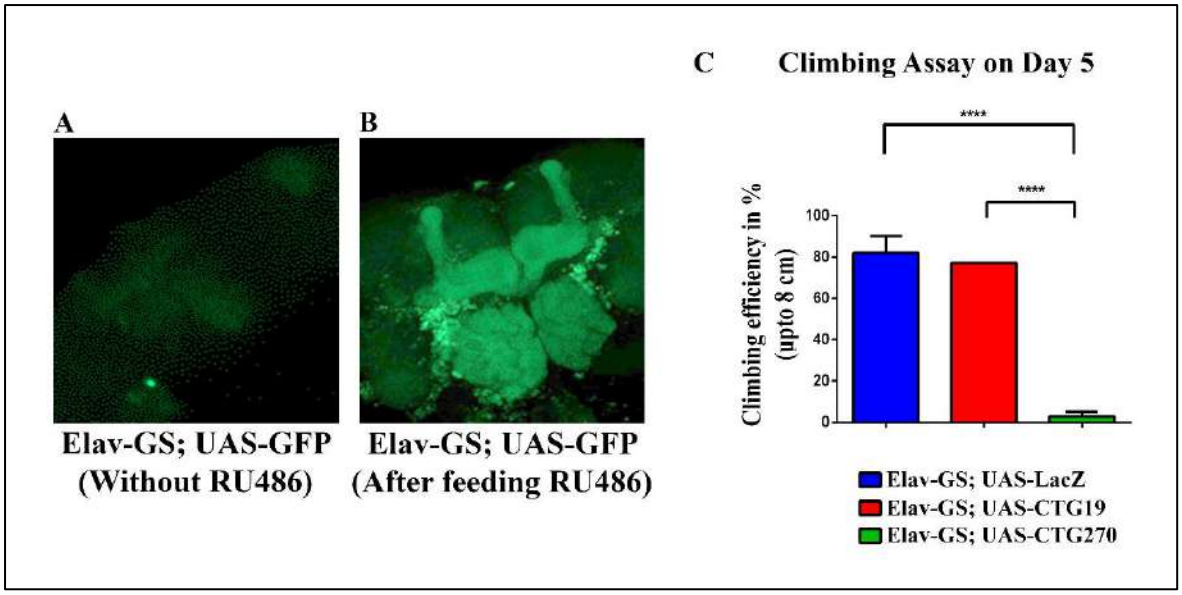

Figure 6: Validation of the Elav-GS Gal4. Elav-GS crossed with UAS GFP, without feeding RU486 (mifepristone), does not show a GFP signal (A). In contrast, another set of flies was fed 100 µg RU486 per 1 mL of food media, which yields a GFP signal (B). (C) Climbing assay with 5-day-old flies using Elav-GS reveals a drastic locomotion defect in flies with CUG repeat expansion, **** $P < 0.0001$. Ordinary One-Way ANOVA with Tukey's Post hoc test has been performed to analyze the climbing efficiency of these flies. Green: GFP. Bar graph represent Mean ± SEM.

3.1.2. CUG-Expanded Repeats Cause Degeneration of the γ Lobe of the Mushroom Body

To investigate the degeneration of mushroom body structure, 201Y-Gal4 was utilized to express CTG270 in the mushroom body. The mushroom body's (MB) role in learning and memory (analogous to the mammalian hippocampus) and composed of Kenyon cells and their axonal projections, namely, α, β, and γ lobes. The Drosophila brain was dissected and stained with neuropile marker FasII to visualise the mushroom body lobes. In control flies, expressing LacZ or non-pathogenic CTG19, the mushroom body lobes were intact at day 10 (Fig. 7A-C). While the α and β lobes remain unaffected, the γ lobe exhibited degeneration in CTG270 expressing flies (Fig. 7A-C). On day 25, complete loss of γ lobes was observed in CTG270 flies, although the control flies did not show any loss of the γ lobe structure (Fig. 7D-F). To quantify the overall volume of the mushroom body

ImageJ software was used. The mean mushroom body volume was 15,000 ± 3000 μm^3 in control flies at day 10. There was a significant reduction in mushroom body structure at day 10 due to the expression of CTG270 (6000 ± 1802 $\mu m^{3)}$ (Fig. 7G). Similarly, at day 25, a drastic reduction in mushroom body volume was observed. Moreover, a significant reduction in mushroom body volume was observed in flies expressing CTG270 on day 10 and day 25 (Fig. 7G).

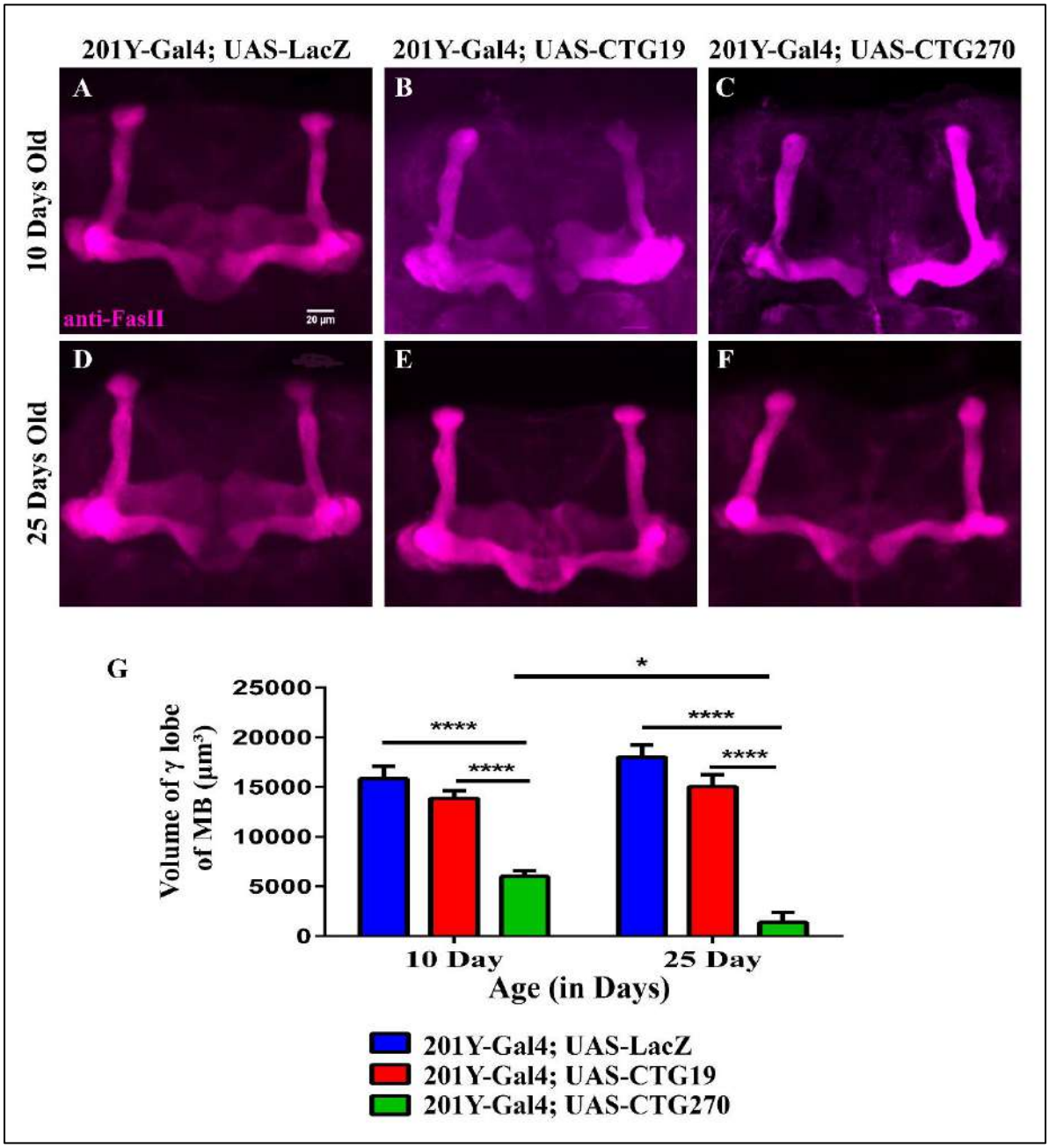

Figure 7: Quantification of γ lobe degeneration at 10 days and 25 days. (A-F) Confocal images of the mushroom body using anti-FasII. (A-C) Representative images of 10-day-old flies of the above-mentioned genotypes. (D-F) Representative images of 25-day-old flies, showing complete degeneration in the γ lobe. (G) Quantification graph

demonstrating the reduction of the volume of the γ lobe, Volume of γ lobe (in μm^3) = Area of ROI * Thickness of a slice * Number of slices, was used to quantify the mushroom body lobes. *p< 0.01, ****p<0.0001, Two-way ANOVA with Sidak's multiple comparison test. Scalebar 20 μm. Magenta: anti-FasII. Bar graph represent Mean ± SEM

3.1.3. Effects Of CUG Repeats on The Dopaminergic Clusters Present In *Drosophila*

To investigate the neurotoxicity in brain dopaminergic neurons (DANs), Ple-Gal4 was used to express CTG270. Ple-Gal4 allows robust expression of the transgenes across the DANs. To investigate the degeneration of dopaminergic neurons, 25-day old adult

The Drosophila brain was dissected and stained with anti-TH antibody (Fig. 8A-I). Notably, widespread neurodegeneration was observed across multiple dopamine (DA) clusters. PAM cluster, which constitutes the largest DAN population in wild-type flies (~110 neurons), exhibited a ~35% reduction in neuronal count (Fig. 8J). In contrast, the smaller DA clusters showed a more severe decline. (Fig. 8G-I), suggesting that CUG toxicity disrupts dopaminergic circuits.

Since the DA neuron regulates behavior and locomotion in flies, we assessed motor ability using a negative geotaxis assay. A significant impairment in climbing ability was evident between 10-day-old and 25-day-old diseased flies ($p < 0.0001$). They exhibited pronounced motor deficits, frequently failing to climb and instead sliding down the assay vials (Fig. 8K).

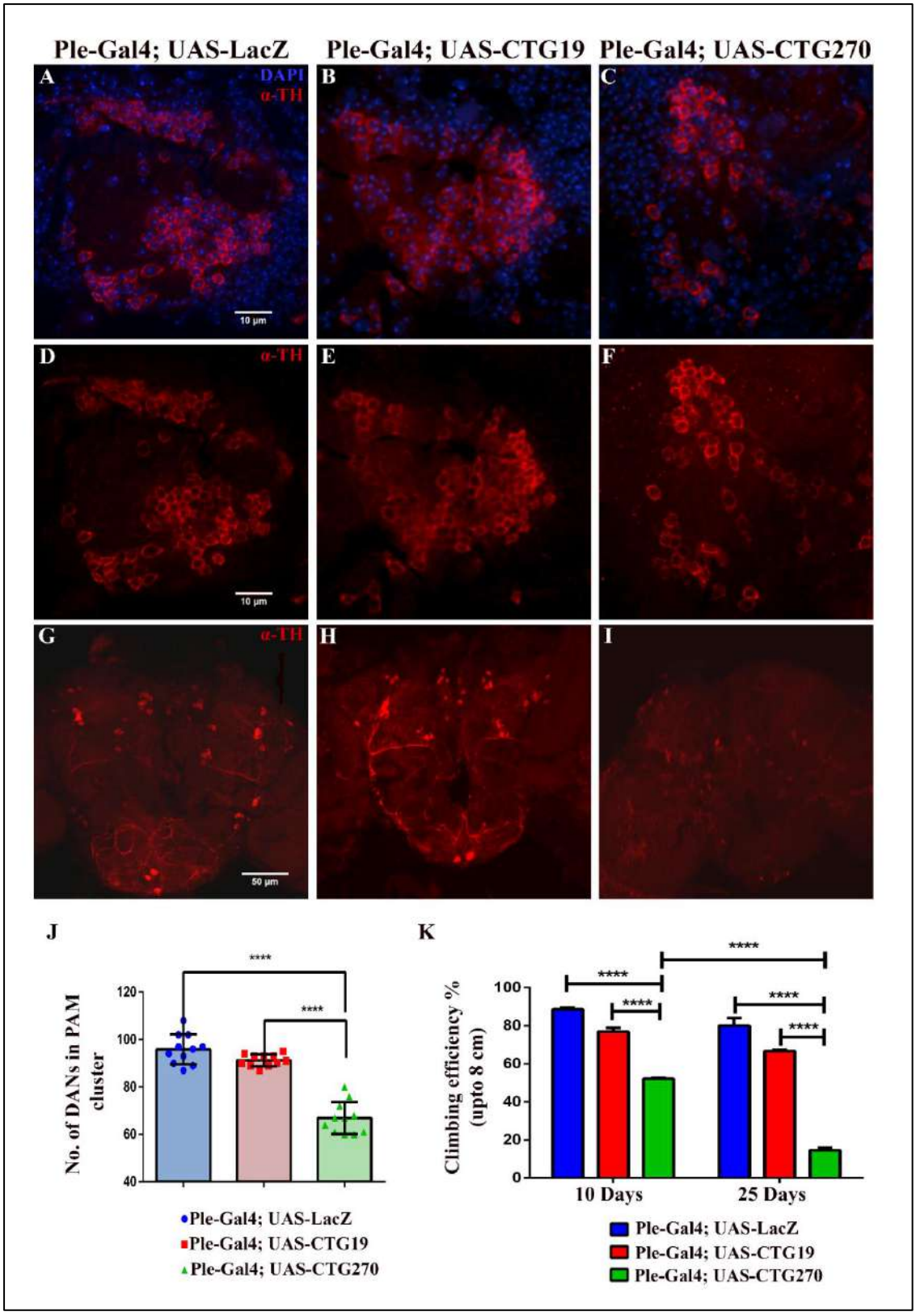

Figure 8: Expression of expanded CUG repeats in dopaminergic neurons results in degeneration and reduction in the DANs cluster. (A-F) Representative confocal Images of PAM cluster of DANs in 25-day-old *Drosophila* with indicated genotypes stained with anti-Tyrosine Hydroxylase (TH). (G-I) Representative confocal image of the

anterior brain marking smaller DA clusters. (A, D, G) Ple-Gal4, UAS-LacZ. (B, E, H) Ple-Gal4; UAS-CTG19. (C, F, I) Ple-Gal4; UAS-CTG270. (J) Bar graph representing the quantification of the number of DAN cells present in the PAM cluster. One-way ANOVA with Tukey's Post hoc was used for statistical analysis, **** $P < 0.0001$. (K) The bar graph shows the number of flies that cross the 8 cm mark at 10-day-old and 25-day-old flies. Scalebar 10 μm (A-F), scalebar 50 μm (G-I). Blue: DAPI, Red: anti-TH. Bar graph represent Mean ± SEM.

3.1.4. Increased CUG Repeats Lead to Toxic RNA-Foci Formation

One of the characteristic features of Myotonic dystrophy is the formation of RNA foci, which sequester RNA-binding proteins, such as MBNL1, which plays a crucial role in splicing [7,8]. Moreover, recent studies have shown the involvement of the brain in DM1 (as mentioned in section 1.1.2). Therefore, we investigated whether expression of abnormally expanded CTG repeats could induce RNA foci formation in the brain. Using the $(CUG)_{10}$ fluorescent probe, we performed Fluorescence In-Situ Hybridization (FISH) to detect RNA foci in adult Drosophila brain. Control flies expressing LacZ, or CTG19, do not show the presence of RNA foci (Fig. 9A-B). However, flies expressing CTG270 showed the presence of abundant cytoplasmic RNA foci, and a few of the foci were localized in the nucleus (Fig. 9C-F).

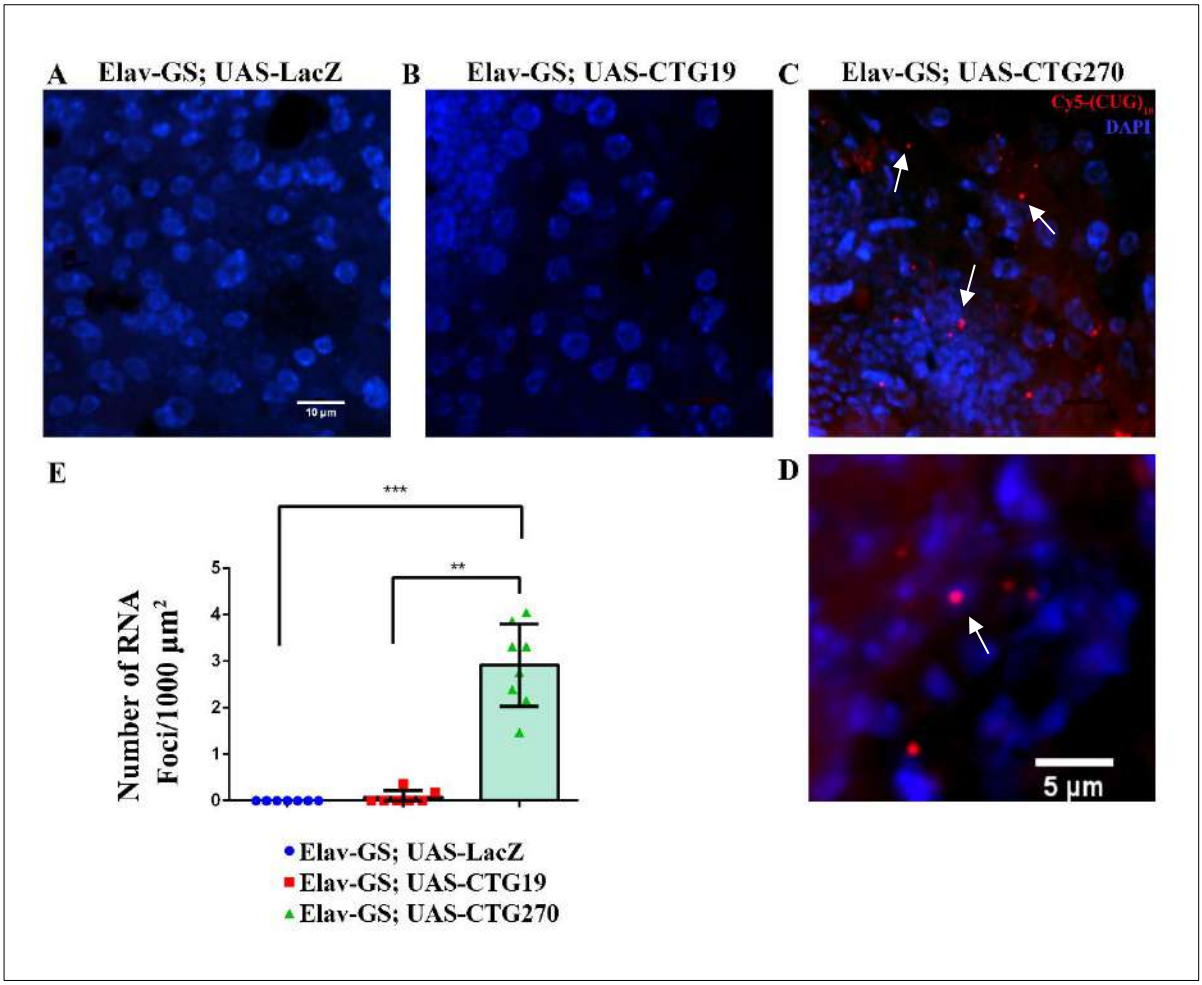

Figure 9: RNA foci are formed in the adult brain. (A-E) RNA foci were detected using a $(CUG)_{10}$ probe labeled with the Cy5 fluorescent dye, and the nucleus was marked with DAPI in 5-day-old flies. (A-B) No RNA foci were detected in flies expressing only LacZ or CTG19. (C-D) RNA foci, which were localized in both the cytoplasm and the nucleus, were observed in CTG270 flies. Scale Bar: 10 µm (D) High magnification at 60X showed nuclear localization of RNA foci. Scalebar: 5µm (F) Bar graph depicting the number of RNA foci present per 1000 µm 2. Kruskal-Wallis Test with Dunn's post hoc was used for comparison, **P < 0.05, ***P < 0.001. (A-D). Blue: DAPI, Red: Cy5-$(CUG)_{10}$. Bar graph represent Mean ± SEM.

3.2. Investigation of the Autophagic Pathway in DM1 Drosophila brain

3.2.1. The expression of autophagy-related genes in adult brain in DM1 flies

Several studies have reported overactivation of the autophagy-lysosome pathway in DM1 models. Increased expression of autophagic markers and apoptotic activation has been

reported in muscle cells in *Drosophila* [52], primary human cell lines from adult-onset DM1 patients [53], and in human DM1 embryonic stem cells-derived neural stem cells [54]. However, the role of autophagy in neuronal tissue and the brain is not well known. We investigated the expression of autophagy-related genes using Elav-GS in the fly brain expressing CTG270. The adult fly heads were decapitated to isolate RNA and prepare cDNA. The real time PCR showed significant upregulation of Atg5, Atg8a and Ref(2)P (the Drosophila ortholog of human p62 protein) (Fig. 10A). However, there is no significant change in the level of Atg12, and Atg1 showed decreased expression in diseased flies compared to control (Fig. 10A). Furthermore, the expression level of Ref(2)P protein using Western blot experiment. Ref(2)P protein was significantly increased in CTG270 flies as compared to control flies expressing GFP and CTG19 (Fig. 10B)

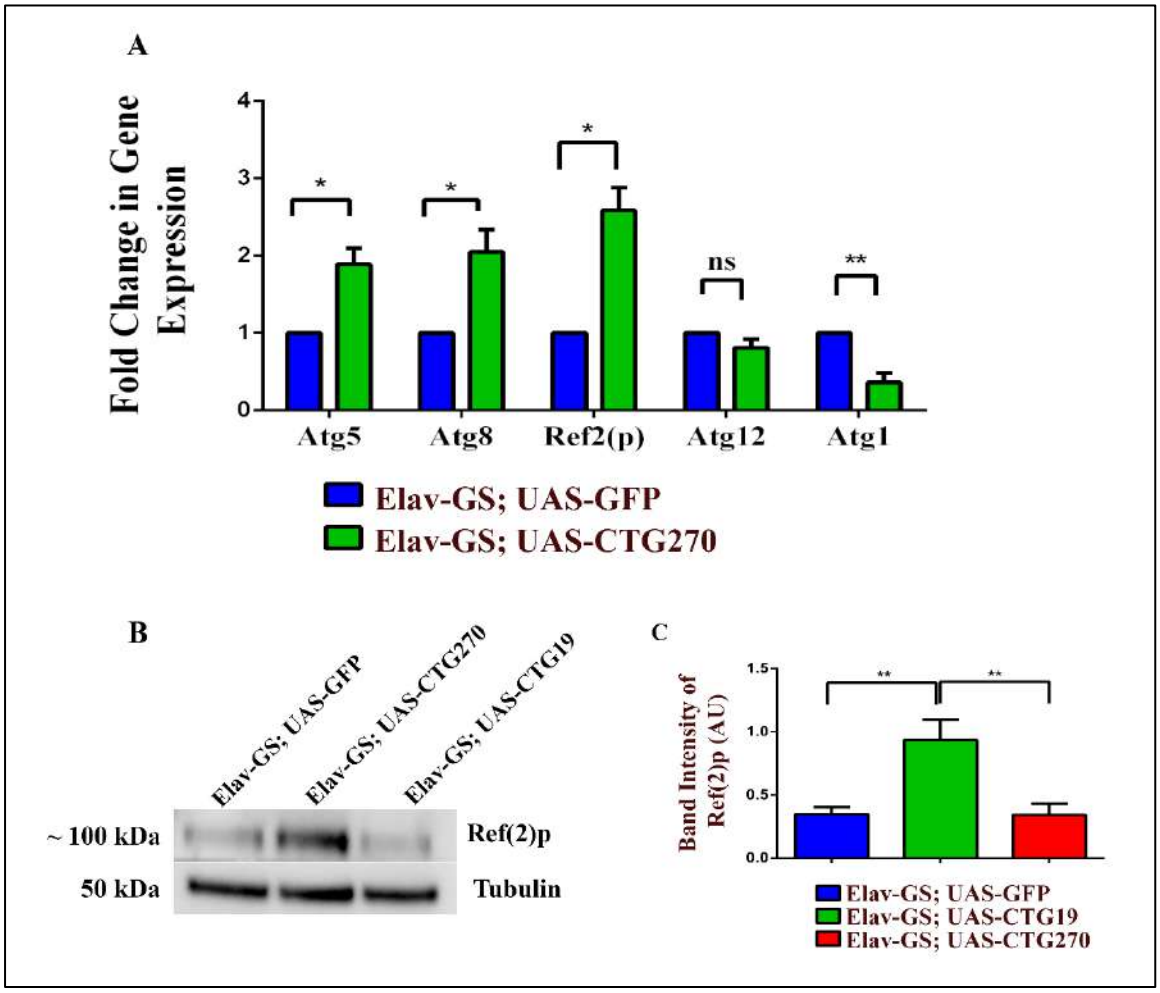

Figure 10: Upregulation of autophagy in the CTG270 expressing fly brain. (A) The expression of autophagy-related genes is upregulated in flies expressing expanded CUG repeats. Fold change in gene expression of Atg1, Atg5, Atg8a, Atg12, and Ref(2)p was measured by qPCR in adult heads. Atg5, Atg8a, Ref(2)p shows upregulation in gene

expression, *p < 0.01, (Mann-Whitney Test). (B) Western blot also demonstrates increased protein expression of Ref(2)p in diseased flies. (C) Quantification of Western blot of Ref(2)p levels observed in indicated genotypes. **p< 0.05, paired t-test. Bar graph represent Mean ± SEM.

4. Discussion

This study demonstrates that the expression of pathogenic CTG270 repeats in *Drosophila melanogaster* leads to neurodegeneration, behavioral deficits, and dysregulated autophagy, recapitulating key features of myotonic dystrophy type 1 (DM1). Our findings highlight the neurotoxic effects of CUG-repeat expansions in distinct neuronal populations, including mushroom body neurons and dopaminergic neurons, and provide insights into the role of autophagy dysregulation in DM1-associated neurodegeneration.

4.1. CTG Repeat Expression in Neuronal Tissues Reduces Longevity and Induces Neurotoxicity

The expression of CTG270 under pan-neuronal (Elav-GS) and tissue-specific drivers (201Y-Gal4, Ple-Gal4, D42-Gal4) resulted in a significant reduction in lifespan. These findings align with the neurotoxic effects observed in mammalian DM1 models, highlighting the sensitivity of neuronal populations to RNA toxicity [52-54]. Notably, pan-neuronal expression of CTG270 (Elav-Gal4) caused larval lethality, suggesting developmental intolerance to CUG-repeat toxicity. In contrast, adult-onset expression (Elav-GS) permitted survival but triggered rapid neurodegeneration and shortened lifespan, indicating age-dependent vulnerability. This observation suggests distinct mechanisms: early lethality may reflect the disruption of neurodevelopmental processes, while adult degeneration likely stems from the accumulation of RNA foci or splicing dysregulation.

4.2. Mushroom Body Degeneration Suggests Targeted Neuronal Vulnerability

Targeted expression of CTG270 in mushroom body neurons, critical for learning and memory in flies, via 201Y-Gal4 led to progressive degeneration of the γ lobe, as evidenced by confocal imaging and volumetric quantification, and displayed selective degeneration of the γ lobe upon CTG270 expression. While the α and β lobes remained intact, the γ lobe was markedly reduced in volume by day 10 and had complete degeneration by day 25, indicating a time-dependent, progressive neurodegeneration. This parallels findings in DM1 patients, where cerebral atrophy and cognitive deficits are common [55-57,69].

4.3. Dopaminergic Neuron Loss and Locomotor Deficits Recapitulate Motor Symptoms

CTG270 expression in dopaminergic neurons (DANs) using Ple-Gal4 resulted in widespread degeneration of multiple DA clusters, with the PAM cluster showing a ~35% reduction in neurons. Smaller DAN clusters were more severely affected, which may explain the motor deficits observed in negative geotaxis assays. Since dopamine regulates locomotion and reward behaviour [49-50,58], these findings align with motor dysfunction and psychiatric symptoms in DM1 patients [59-62].

4.4. RNA Foci Formation Confirms Molecular Signature of DM1

A hallmark of DM1 pathology is the formation of nuclear RNA foci, which sequester RNA-binding proteins such as MBNL1 and disrupt alternative splicing [67,68 9,10]. Our FISH experiments confirmed that CTG270 expression in the adult brain results in cytoplasmic and nuclear RNA foci, which are absent in control genotypes. This confirms that the Drosophila model faithfully recapitulates molecular features of DM1 and reinforces the pathogenic role of repeat-expanded RNA.

4.5. Dysregulation of Autophagy Highlights a Key Mechanism of Neuronal Dysfunction

Autophagy, a cellular degradation, and recycling pathway was markedly altered in the CTG270-expressing brain. Intriguingly, we found significant upregulation of autophagy markers Atg5, Atg8a, and Ref(2)p at the transcript level, and accumulation of Ref(2)p protein, indicating a block in autophagic flux or impaired autophagic clearance due to defective clearance of toxic RNA-protein aggregates, consistent with reports in DM1 muscle system [63-65]. Interestingly, Atg1 was downregulated, suggesting early-stage autophagy initiation might be compromised. The accumulation of Ref(2)p, a homolog of human p62, further supports impaired autophagic degradation—a phenomenon linked to multiple neurodegenerative conditions, including Alzheimer's and Parkinson's diseases. These findings suggest that dysregulated autophagy could be a central contributor to neuronal dysfunction in DM1 and a potential therapeutic target.

4.6. Limitations and Future Directions

While this study establishes the neurotoxic effects of CUG repeats in *Drosophila,* translating these findings into therapeutic strategies requires addressing key limitations. Specifically,

The dual role of autophagy: We have already observed that autophagy is upregulated (Atg5, Atg8a, Ref(2)p) in the disease. However, it is unclear whether this response is protective, leading to the clearance of toxic RNA foci, or whether it causes impaired autophagy, resulting in cell death, as Ref(2)p accumulation suggests impaired flux [66].

No rescue experiments were conducted: We found upregulation in autophagy gene expression, which raises the question of whether autophagy modulators or RNA inhibition of Atg genes can alleviate the disease phenotypes.

Mechanism of Neurodegeneration: In this study, we focused solely on the autophagy pathway; the roles of oxidative stress, mitochondrial dysfunction, or mitophagy have yet to be explored.

5. Materials and Methods:

- **Nutrient Medium:**

Requirement: Water, 0.55% Agar, 4.72% Maize Powder, 4.16% Sugar, 1.66% Yeast, 0.27% Nipagin, 0.277% Propionic Acid

Procedure: To prepare the cornmeal media, agar is added to the water and boiled until it becomes transparent. Once the agar becomes transparent, a paste is prepared using maize powder, sugar, yeast, and nipagin, which is then added. Thereafter, the mixture is boiled to achieve a sticky consistency while stirring continuously. Propionic acid is added once the food has cooled. The food is then portioned into vials and bottles. Once the food solidifies, the bottles and vials are plugged using cotton balls.

- **Stock Maintenance:**

Table 1: Types of containers

Container Type	Media Volume	Common Use
Small vials	2 mL	Virgin collection, male-female fly separation
Regular vials	6 mL	Stock maintenance, long-term storage, experimental cross setup,
Bottles	18 mL	Mass rearing for behavioural assays and large-scale experiments

- **Drosophila Stocks:**

Most of the transgenic lines used for this dissertation project were purchased and further reared from the Bloomington Drosophila Stock Center. Based on experimental requirements, a few recombinant lines have been generated in the lab. Table 2 provides a detailed list.

Table 2: Transgenic lines used during experiments

BDSC Stock Number	Stock	Chromosome Number	Description
1776	+; UAS-LacZ; +	2	Expresses LacZ under the control of UAS
-	UAS-GFP	2	Expresses GFP under the control of UAS
-	Wild Type		
8848	Ple-Gal4	3	Expresses GAL4 in dopaminergic cells
4440	201y-Gal4;+	2	Expresses GAL4 in the Mushroom Body
43642	Elav-GS	3	Expresses steroid activated GAL4 in neurons.
79581	w[1118]; P{w[+mC]=UAS-DsRed-CTG270}13.1	2	Expresses dsRed under the control of UAS with 270 uninterrupted CTG repeats.
8765	elav-Gal4/CyO; dCo2/TM6B	2,3	Expresses GAL4 pan-neuronally.
8848	w[*]; P{w[+mC]=ple-GAL4.F}3	3	Expresses GAL4 in dopaminergic cells
79576	w[1118]; P{w[+mC]=UAS-DsRed-CTG19}1.1	3	Expresses dsRed under the control of UAS with 19 uninterrupted CTG repeats.
51656	P{ry[+t7.2]=hsFLP}1, y[1] w[1118]; P{w[+mC]=UAS-Atg8a.GFP}3	3	Expresses GFP-tagged Atg8a protein under UAS control.

- **Crossbreeding Setup:**

Virgin females of one genotype and male flies of another genotype are paired in a bottle in a 1:1 ratio (approximately 10 flies each) to initiate crossbreeding. All the experimental crosses and flies are kept at 25°C.

- **Dissection Protocol:**

Solutions required:

a. 10x PBS: NaCl (130mM) – 76.05g, Na_2HPO_4 (7mM) – 12.46g, NaH_2PO_4 (3mM) – 4.68g, make upto 1L using autoclaved distilled water. The pH is adjusted to 7.4.
   For 1x PBS, 100 mL of 10x PBS is diluted in 900 mL of autoclaved water.
b. 1x PBST: 1x PBS with 0.1% Triton X-100
c. 4% PFA: 250 µL of 16% paraformaldehyde (PFA) dissolved in 750 µL of 1x PBS.
d. Blocking Solution: 0.1% Bovine Serum Albumin (BSA) in PBST.

Procedure:

Adult flies are anesthetized for 30 seconds before decapitation using two fine needles. The proboscis is removed from the head in 1x PBS. Subsequently, the samples are fixed in a 4% PFA solution for 1 hour, followed by Three Washes with PBST, each for 10 minutes. To separate the brain from the head, first, a needle is positioned underneath the proboscis, and then the retinal region is removed with another needle. The upper exoskeleton is gently removed to expose the brain, and the brain is carefully pushed out of the exoskeleton. Thereafter, the trachea is removed from the periphery without damaging the sample using the tip of the needle. The samples are kept in a cavity block containing 1x PBS.

The dissection process to visualize the dopaminergic neuron cluster present in the brain is slightly different. The blocking solution in this case consists of 0.5% PBST (1x PBS, 0.5% Triton X 100) and 10% BSA. The trachea surrounding the brain must be removed entirely for better penetration of antibodies.

- **Fluorescence In Situ Hybridization:**

Requirement: 50% Formamide, 5x SSC, 0.1% Tween 20, Herring Sperm DNA, Nuclease-free Water

PBST, Methanol, 4% PFA, Glycine, Hybridization Solution, RNA Probe, DAPI Stain.

Hybridization Solution: 50% Formamide, 5x SSC, 0.1% Tween 20, Herring Sperm DNA, Nuclease-free Water

Pre-Hybridization Solution: 200 µL of hybridization per genotype is boiled at 95°C in dry heat for 5 minutes, then cooled in ice for 5 minutes.

Procedure:

1. The fly brain is dissected according to the dissection protocol.
2. The samples are rinsed with methanol and again rinsed with 200 µL methanol and PBST (1:1 ratio)
3. The samples are washed with 200 µL PBST for 2 minutes, twice.
4. Samples are fixed with 4% PFA for 20 minutes.
5. Samples are washed with 200 µL PBST for 2 minutes, three times.
6. Samples are given PBST and 2mg/mL glycine washes for 2 minutes, twice.
7. Samples are rinsed with PBST and hybridization solution (1:1 ratio).
8. The solution is removed, and 200 µL hybridization solution is added to the sample for 5 minutes.
9. 200 µL of pre-hybridization solution is added to the samples, which are then incubated for 2 hours at 56°C in a water bath.
10. For each genotype, 2 µL of RNA probe and 200 µL of hybridization solution are boiled in a vial at 80°C for 3 minutes, then cooled in ice for 5 minutes.
11. The probe solution is then added to the samples and incubated at 56°C for 16 hours in a dark condition.
12. A. Hybridization solution
    B. A solution with hybridization solution and PBST (3:1 ratio)
    C. A solution with hybridization solution and PBST (1:1 ratio)
    D. A solution with hybridization solution and PBST (1:3 ratio)
    E. PBST
    A-E is prepared in vials and warmed at 56°C beforehand.
13. Once the incubation period is over the samples are taken out and rinsed with pre-warmed solution A
14. Next, the samples are washed with 200 µL of solutions A to D for 15 minutes each at 56°C.
15. The samples are washed with solution E for 5 minutes, 4 times, maintaining the 56°C temperature.
16. The samples are then brought to room temperature and stained with DAPI solution for 45 minutes.

17. The samples are mounted on a slide and imaged in a confocal microscope.

- **Immunostaining:**

The previously dissected samples are fixed in 4% PFA for 30 minutes, followed by a 16-hour incubation with primary antibody in cavity block at 4°C. These samples are washed three times with PBST for 10 minutes each. Next, they are incubated in fluorophore-conjugated secondary antibody for 2 hours in the dark. The samples are washed with PBST thrice, before mounting on the slide using a spacer, Vectashield mounting media (Vector Laboratories), and imaged using a Nikon Confocal Microscope (Model A1 HD25, FOV of 25 mm, Tokyo; Model AXR, 25 mm FOV resonant scanner, 25 mm FOV Galvano scanner), using Nikon NIS-Elements C software.

The immunostaining protocol differs for dopaminergic neurons, as the samples are incubated with the primary antibody for 72 hours at 4°C, and the incubation period for the secondary antibody is 24 hours. The wash period increases for 15 minutes, 4 times after each incubation.

Antibodies used:

Antibody	**Catalogue**	**Host Model**	**Dilution**	**Use**
Anti Fasciclin II	DSHB/1D4	mouse	1:20	IF
Tyrosine Hydroxylase	Sigma/AB152	Rabbit	1:100	IF
GFP	CST/2956S	Rabbit	1:100	IF
GFP	DSHB/12A6	mouse	1:100	IF
Alexa 488 anti-mouse	A-11001/Thermo	Goat	1:200	IF
Alexa 647 anti-mouse	A-31571/Thermo	Donkey	1:200	IF
Alexa 647 anti-rabbit	A-21245/thermo	Goat	1:200	IF
Alexa 546 anti-rabbit	A-11035/Thermo	Goat	1:200	IF

- **Negative Geotactic Assay:**

The Climbing Assay, also known as the negative geotaxis assay, is a behavioral assay used to assess locomotion abilities and age-related decline in *Drosophila*. This assay utilizes the natural tendency of flies to climb upward against gravity. To perform this assay, 10 adult flies

of the same age (10 days old and 25 days old) are introduced to the climbing ring assay test vials with a threshold of 8 cm marked. After 5 minutes of acclimatization, the vial is gently tapped to bring the flies to the bottom, and the number of flies capable of crossing the threshold within 10 seconds is recorded. Three consecutive readings are performed using the same flies, with a 1-minute interval between each reading. Fifty flies for each genotype have been studied.

- **Survival Assay:**

Male and female pupae are collected and separated in different vials. Once they emerge, ten flies are placed in each vial, with six vials (n = 60). The flies are transferred into a new vial every day, and the number of dead flies is recorded until all the flies have died. The Kaplan-Meier test is used to generate statistical data, and a survival plot is formed using GraphPad Prism 6.

- **Drug dosage for Elav GS**

A stock solution of mifepristone (Sigma) was prepared at a concentration of 1 mg/mL in ethanol. To activate the Elav-GS Gal4 line, a working concentration of 100 µg/mL mifepristone was diluted in food media. Flies were maintained on the mifepristone-containing food, with vials replaced every 48 hours to ensure consistent drug exposure.

- **RNA isolation:**

Requirement: Trizol reagent, Chloroform, Isopropanol, 70% Ethanol, Nuclease-free Water (NFW), DEPC

Trizol Method:

1. **Tissue Lysis:**
   A. The fly heads are decapitated and transferred to a centrifuge tube.
   B. 200 µL of trizol is added to the sample.
   C. The samples are homogenized using disposable plastic pestles and are incubated at room temperature.
2. **Phase separation:**
   A. 100 µL of chloroform is added and shaken vigorously, mixed upside-down for 10 seconds.

B. The sample is centrifuged at 12000 rpm for 20 minutes at 4°C.
C. Once three phases are separated, the upper aqueous phase containing RNA is collected into a fresh tube without disturbing the interphase.

3. **Isolation of RNA Pellet:**
   A. Isopropanol is added to the aqueous phase, and the sample is allowed to stand for 30 minutes at room temperature.
   B. The samples are centrifuged for 20 minutes at 12000 rpm at 4°C. The RNA pellet can be found on the side or the bottom of the centrifuge tube.
   C. The supernatant is discarded, and the RNA pellet is washed with 200 µL of 75% ethanol diluted with DEPC.
   D. The sample is centrifuged at 4°C for 5 minutes.
   E. The ethanol solution is discarded, and the sample is left to air dry for 15 minutes.
   F. 20 µL of NFW is added to the pellet and stored in the -80°C until cDNA formation.

- **RNA Quantification by NanoDrop Spectrophotometer:**

RNA concentration and purity are determined using a NanoDrop spectrophotometer. One µL of the RNA sample is used to determine the concentration of the RNA. Absorbance at 260 nm is used to determine RNA concentration, while purity is assessed using A260/A280 and A260/A230 ratios.

- **First Strand cDNA synthesis:**

1 µg of the total RNA was reverse transcribed to first-strand cDNA using the iScript cDNA Synthesis Kit.

Table 6: Reaction set up for the first strand cDNA synthesis.

Total RNA	1 µg
Reaction Mix	4 µL
Reverse Transcriptase Enzyme	1µL
Nuclease-free Water	Make upto 20 µL
Total volume	20 µL

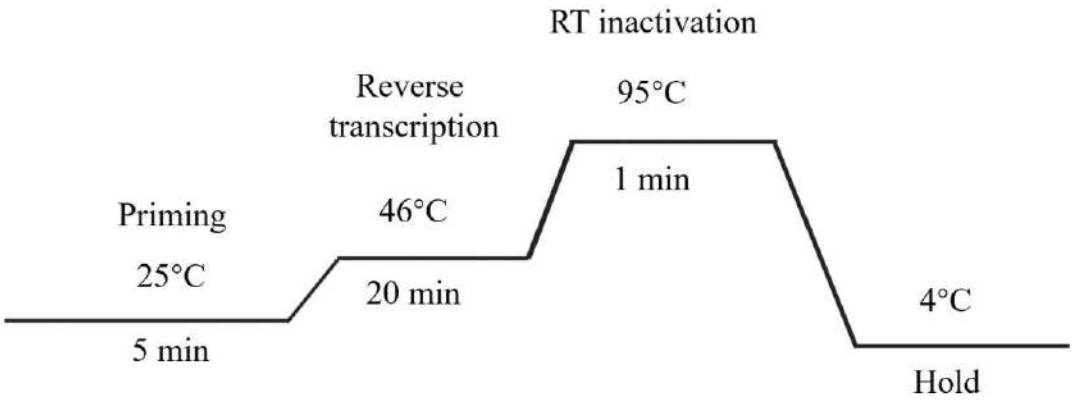

Fig. 6: Thermal cycling conditions for the amplification of the genes. It was performed in a Thermocycler.

- **Real-time PCR Analysis:**

Real-time PCR was performed using SYBR Green with the following primers:

Table 7: Sequences of the primer pairs and their product size

Primer	**Sequence**
RP49	Forward 5'TTCTACCAGCTTCAAGATGAC3' Reverse 5'GTGTATTCCGACCACGTTACA3'
ATG1	Forward 5'CGTCTACAAAGGACGTCATCGCAAGAAAC3' Reverse 5'CGCCAAGTCGCCGCCATTGCAATACTC3'
ATG5	Forward 5'CCTGCGAATCTATACAGACGATGAC3' Reverse 5'AGCTCAGATGCTCGGACATCCATTG3'
ATG8a	Forward 5'TCGCAAATATCCAGACCGTGTGCCCGTC3' Reverse 5'GCCGATGTTGGTGGAATGACGTTGTTCAC3'

Primer	Sequence
ATG12	Forward 5’GCCAGCGAGCAAATTTTCCT3’ Reverse 5’GCAAAGTCATGTGCGTATCGA3’
Ref(2)P	Forward 5’CGTAAGGACCTTCTGGATCG3’ Reverse 5’GTGCATATTGCTCTCGCACT3’

RP49 is used as an endogenous control. Real-time PCR was performed using SYBR Green in Bio-Rad Real-time PCR.

Table 8: Reaction set up for Real-time PCR

Template (cDNA)	1 µL
SyBR Green Master Mix	5 µL
Forward Primer	0.3 µL
Reverse Primer	0.3 µL
Nuclease Free Water	Make up to 10 µL

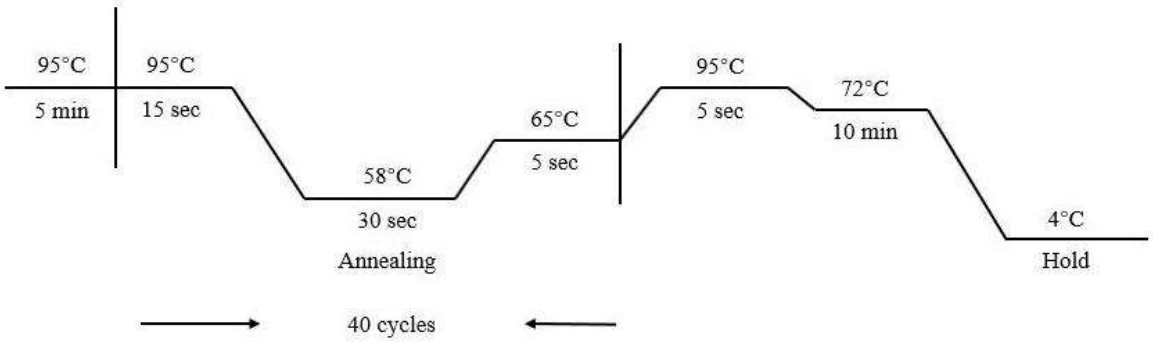

Fig. 7: Thermal cycling conditions for the amplification of the genes. It was performed in the Bio-Rad CFX Opus Real-Time PCR System.

- **Western Blot:**

Table 9: Antibodies used for Western blot

Antibody	Catalogue	Host Model	Dilution	Use
Ref(2)p	Abcam/ab178440	Rabbit	1:5000	WB
GAPDH	DHSB	Mouse	1:5000	WB
DCP1	CST/9578S	Rabbit	1:1000	WB
Actin	DSHB/JLA20	Mouse	1:2000	WB
Beta tubulin	DSHB/E7	Mouse	1:2000	WB

By using the antibodies mentioned above, proteins related to autophagy pathway and cell death are detected through western blot technique.

A. Sample preparation:

1. 40 heads per genotype are lysed using RIPA buffer with protease inhibitor cocktail.
2. The samples are centrifuged to remove debris.
3. The protein sample is quantified using the BCA assay.

B. Gel electrophoresis:

1. An SDS-PAGE gel with a 12% resolving gel and a 5% stacking gel is prepared.
2. Protein ladder and 20 µg of each protein sample, mixed with loading dye are loaded.
3. The gel is run at 60V for the stacking gel and 120V for the resolving gel until the dye front reaches the bottom.

C. Protein transfer and blocking:

1. Protein samples are transferred using a nitrocellulose membrane or a PVDF membrane activated with methanol.
2. Once transferred, the membrane is incubated in 5% skimmed milk in PBST (PBS and 0.1% Tween 20) for 1.5 hours in RT.

D. Primary and secondary antibody incubation:

1. Primary antibody is diluted in blocking buffer in 1;1000 dilution and incubated for 16 hours at 4°C.
2. The membrane is washed with PBST, 3 times, 10 minutes each.

3. The membrane is incubated with HRP-conjugated secondary antibody (1:5000 dilution in blocking solution) for 2 hours in RT.
4. The blots are washed with PBST for 10 minutes, 3 times.
5. The blots are then imaged using ECL substrate in the Uvitech-Chemi Imager apparatus.

- **Image Processing and Image Analysis:**

Images are collected using Nikon Confocal A1 HD25 and Confocal AXR microscopes. Raw confocal images are converted into a TIFF file format using NIS-Elements AR software and analyzed using Fiji ImageJ. Images have been taken in 40x and 60 objectives.

For RNA foci puncta analysis, the image is stacked and converted to an 8-bit type. Otsu thresholding has been applied to the image, and then to count the puncta, the 'Analyze Particles' function has been used.

To measure the DANs cell count, the 'cell counter' plug-in is used. This is a semi-automatic facility to count cells according to its type.

- **Statistical Analysis:**

All statistical analyses are performed using GraphPad Prism 6.0 software (GraphPad Software, 2014). All results are presented as mean ± SEM, providing a range within which the true sample mean is likely to fall. The assumption of normal distribution is measured with the Shapiro-Wilk test, and the homogeneity is checked with Bartlett's test. All climbing assays and the number of DANs are quantified using an Ordinary One-way ANOVA test with Tukey's post hoc analysis. Volume of γ lobe is quantified using Two-way ANOVA with Sidak's multiple comparison test. The Kruskal-Wallis test, along with Dunn's post hoc analysis (for RNA foci count) and the Mann-Whitney test (for fold-change in Autophagy-related gene expression), were used for analysis.

For the survival graph, the Kaplan-Meier method, a non-parametric statistical analysis along with the Log-rank test is used to determine significance between different genotypes.

References

1. De Antonio M, Dogan C, Hamroun D, Mati M, Zerrouki S, Eymard B, Katsahian S, Bassez G, Network FM. Unravelling the myotonic dystrophy type 1 clinical spectrum: a systematic registry-based study with implications for disease classification. Revue neurologique. 2016 Oct 1;172(10):572-80
2. Pratte A, Prévost C, Puymirat J, Mathieu J. Anticipation in myotonic dystrophy type 1 parents with small CTG expansions. American Journal of Medical Genetics Part A. 2015 Apr;167(4):708-14.
3. Martorell L, Cobo AM, Baiget M, Naudó M, Poza JJ, Parra J. Prenatal diagnosis in myotonic dystrophy type 1. Thirteen years of experience: implications for reproductive counselling in DM1 families. Prenatal Diagnosis: Published in Affiliation With the International Society for Prenatal Diagnosis. 2007 Jan;27(1):68-72.
4. Bundey S. Clinical evidence for heterogeneity in myotonic dystrophy. J Med Genet. 1982;19(5):341–8. https://doi.org/10.1136/jmg.19.5.341.
5. Dogan C, Antonio MD, Hamroun D, Varet H, Fabbro M, Rougier F, et al. Gender as a Modifying Factor Influencing Myotonic Dystrophy Type 1 Phenotype Severity and Mortality: A Nationwide Multiple Databases Cross-Sectional Observational Study. PLOS ONE. 2016;11(2):e0148264. https://doi.org/10.1371/journal.pone.0148264.
6. Han JY, Jang W, Park J. Intergenerational Influence of Gender and the DM1 Phenotype of the Transmitting Parent in Korean Myotonic Dystrophy Type 1. Genes. 2022;13(8):1465. https://doi.org/10.3390/genes13081465.
7. Chun-Ho W, Lien N, Jessie P, Tiziano T, Ho T, Yee CW, Edwin CH. Targeting Toxic RNAs that Cause Myotonic Dystrophy Type 1 (DM1) with a Bisamidinium Inhibitor.
8. Cooper TA. Chemical reversal of the RNA gain of function in myotonic dystrophy. Proceedings of the National Academy of Sciences. 2009 Nov 3;106(44):18433-4.
9. Kanadia RN, Johnstone KA, Mankodi A, Lungu C, Thornton CA, Esson D, Timmers AM, Hauswirth WW, Swanson MS. A muscleblind knockout model for myotonic dystrophy. science. 2003 Dec 12;302(5652):1978-80.
10. Du H, Cline MS, Osborne RJ, Tuttle DL, Clark TA, Donohue JP, Hall MP, Shiue L, Swanson MS, Thornton CA, Ares Jr M. Aberrant alternative splicing and extracellular matrix gene expression in mouse models of myotonic dystrophy. Nature structural & molecular biology. 2010 Feb;17(2):187-93.

11. Chau A, Kalsotra A. Developmental insights into the pathology of and therapeutic strategies for DM1: Back to the basics. Developmental Dynamics. 2015 Mar;244(3):377-90.
12. Yu Z, Teng X, Bonini NM. Triplet repeat–derived siRNAs enhance RNA–mediated toxicity in a Drosophila model for myotonic dystrophy. PLoS genetics. 2011 Mar 17;7(3):e1001340.
13. Zu T, Cleary JD, Liu Y, Bañez-Coronel M, Bubenik JL, Ayhan F, Ashizawa T, Xia G, Clark HB, Yachnis AT, Swanson MS. RAN translation regulated by muscleblind proteins in myotonic dystrophy type 2. Neuron. 2017 Sep 13;95(6):1292-305.
14. Moxley RT, Corbett AJ, Minaker KL, Rowe JW. Whole body insulin resistance in myotonic dystrophy. Annals of Neurology: Official Journal of the American Neurological Association and the Child Neurology Society. 1984 Feb;15(2):157-62
15. Peterson JA, Cooper TA. Clinical and molecular insights into gastrointestinal dysfunction in myotonic dystrophy types 1 & 2. International journal of molecular sciences. 2022 Nov 26;23(23):14779.
16. Peric S, Bjelica B, Bozovic I, Pesovic J, Paunic T, Banovic M, Brkusanin M, Aleksic K, Basta I, Pavicevic DS, Stojanovic VR. Fatigue in myotonic dystrophy type 1: a seven-year prospective study. Acta Myologica. 2019 Dec 1;38(4):239.
17. Green HJ, Fraser IG, Ranney DA. Male and female differences in enzyme activities of energy metabolism in vastus lateralis muscle. Journal of the neurological sciences. 1984 Sep 1;65(3):323-31.
18. Welle S, Tawil R, Thornton CA. Sex-related differences in gene expression in human skeletal muscle. PloS one. 2008 Jan 2;3(1):e1385.

19. Hamilton, M. J., McLean, J., Cumming, S., Ballantyne, B., McGhie, J., Jampana, R., ... & Farrugia, M. E. (2018). Outcome measures for central nervous system evaluation in myotonic dystrophy type 1 may be confounded by deficits in motor function or insight. *Frontiers in neurology*, *9*, 780. https://doi.org/10.3389/fneur.2018.00780.
20. Damian MS, Schilling G, Bachmann G, Simon C, Stöppler S, Dorndorf W. White matter lesions and cognitive deficits: relevance of lesion pattern? Acta Neurol Scand. 1994;90(6):430–6. https://doi.org/10.1111/j.1600-0404.1994.tb02753.x
21. Censori B, Provinciali L, Danni M, Chiaramoni L, Maricotti M, Foschi N, et al. Brain involvement in myotonic dystrophy: MRI features and their relationship to clinical and

cognitive conditions. Acta Neurol Scand. 1994;90(3):211–7. https://doi.org/10.1111/j.1600-0404.1994.tb02708.x.

22. Modoni A, Silvestri G, Pomponi MG, Mangiola F, Tonali PA, Marra C. Characterization of the pattern of cognitive impairment in myotonic dystrophy type 1. Arch Neurol. 2004;61(12):1943–7. https://doi.org/10.1001/archneur.61.12.1943.
23. Spaendonck KPM, Bruggen JT, Banningh EW, Maassen BAM, van de B, M. JB, et al. Cognitive function in early adult and adult onset myotonic dystrophy. Acta Neurol Scand. 1995;91(6):456–61. https://doi.org/10.1111/j.1600-0404.1995.tb00446.x
24. Chong-Nguyen C, Wahbi K, Algalarrondo V, Bécane HM, Radvanyi-Hoffman H, Arnaud P, et al. Association between mutation size and cardiac involvement in myotonic dystrophy type 1: an analysis of the DM1-heart registry. Circ Cardiovasc Genet. 2017;10(3):001526. https://doi.org/10.1161/CIRCGENETICS.116.001526.
25. Petri H, Vissing J, Witting N, Bundgaard H, Køber L. Cardiac manifestations of myotonic dystrophy type 1. Int J Cardiol. 2012;160(2):82–8. https://doi.org/10.1016/j.ijcard.2011.08.037.
26. Allen J. Pulmonary complications of neuromuscular disease: A respiratory mechanics perspective. Paediatr Respir Rev. 2010;11(1):18–23. https://doi.org/10.1016/j.prrv.2009.10.002.
27. Lo Mauro A, Aliverti A. Physiology of respiratory disturbances in muscular dystrophies. Breathe. 2016;12(4):318–27. https://doi.org/10.1183/20734735.012716.
28. Ouyang L, Wang Y, Valdez R, Johnson N, Gutmann L, Street N, et al. Gender difference in clinical conditions among hospitalized adults with myotonic dystrophy. Muscle Nerve. 2019;59(3):348–53. https://doi.org/10.1002/mus.26402.
29. Wenninger S, Montagnese F, Schoser B. Core Clinical Phenotypes in Myotonic Dystrophies. Front Neurol. 2018 May 2;9:303. https://doi.org/10.3389/fneur.2018.00303
30. Voermans NC, Erasmus CE, Ockeloen CW, Engelen BG, Eggink CA. Primary cataract as a key to recognition of myotonic dystrophy type 1. Eur J Ophthalmol. 2015;25(4):46–9. https://doi.org/10.5301/ejo.5000565.
31. Cobo AM, Poza JJ, Blanco A, Munain AL, Saénz A, Azpitarte M, et al. Frequency of myotonic dystrophy gene carriers in cataract patients. J Med Genet. 1996;33(3):221–3. https://doi.org/10.1136/jmg.33.3.221.
32. Dahlqvist, J. R., Ørngreen, M. C., Witting, N., & Vissing, J. (2014). *Endocrine function over time in patients with myotonic dystrophy type 1. European Journal of Neurology, 22(1), 116–122.* doi:10.1111/ene.12542

33. Matsumura T, Iwahashi H, Funahashi T, Takahashi MP, Saito T, Yasui K, Saito T, Iyama A, Toyooka K, Fujimura H, Shinno S. A cross-sectional study for glucose intolerance of myotonic dystrophy. Journal of the neurological sciences. 2009 Jan 15;276(1-2):60-5.
34. Antonini G, Clemenzi A, Bucci E, et al. Hypogonadism in DM1 and its relationship to erectile dysfunction. J Neurol 2011; 258: 1247–1253.
35. Hilbert JE, Barohn RJ, Clemens PR, Luebbe EA, Martens WB, McDermott MP, Parkhill AL, Tawil R, Thornton CA, Moxley III RT, National Registry Scientific Advisory Committee/Investigators. High frequency of gastrointestinal manifestations in myotonic dystrophy type 1 and type 2. Neurology. 2017;89(13):1348-54. https://doi.org/10.1212/WNL.0000000000004420.
36. Coërs C, Telerman-Toppet N, Gerard JM. Terminal innervation ratio in neuromuscular disease: II. Disorders of lower motor neuron, peripheral nerve, and muscle. Archives of neurology. 1973 Oct 1;29(4):215-22.
37. Weijs R, Okkersen K, van Engelen B, Küsters B, Lammens M, Aronica E, Raaphorst J, van Cappellen van Walsum AM. Human brain pathology in myotonic dystrophy type 1: A systematic review. Neuropathology. 2021 Feb;41(1):3-20.
38. Tahraoui-Bories, Julie et al. “MBNL-dependent impaired development within the neuromuscular system in myotonic dystrophy type 1.” *Neuropathology and applied neurobiology* vol. 49,1 (2023): e12876. doi:10.1111/nan.12876
39. Kim YK, Mandal M, Yadava RS, Paillard L, Mahadevan MS. Evaluating the effects of CELF1 deficiency in a mouse model of RNA toxicity. Human molecular genetics. 2014 Jan 15;23(2):293-302.
40. Coërs C, Telerman-Toppet N, Gerard JM. Terminal innervation ratio in neuromuscular disease: II. Disorders of lower motor neuron, peripheral nerve, and muscle. Archives of neurology. 1973 Oct 1;29(4):215-22.
41. Krishnan AV, Kiernan MC. Axonal function and activity-dependent excitability changes in myotonic dystrophy. Muscle & Nerve: Official Journal of the American Association of Electrodiagnostic Medicine. 2006 May;33(5):627-36.
42. Wheeler TM, Krym MC, Thornton CA. Ribonuclear foci at the neuromuscular junction in myotonic dystrophy type 1. Neuromuscular Disorders. 2007 Mar 1;17(3):242-7.
43. Laforce RJ, Dallaire-Théroux C, Racine AM, Dent G, Salinas-Valenzuela C, Poulin E, Cayer AM, Bédard-Tremblay D, Rouleau-Bonenfant T, St-Onge F, Schraen-Maschke S. Tau positron emission tomography, cerebrospinal fluid and plasma biomarkers of

neurodegeneration, and neurocognitive testing: an exploratory study of participants with myotonic dystrophy type 1. Journal of Neurology. 2022 Jul;269(7):3579-87.

44. Lin S. The making of the Drosophila mushroom body. Frontiers in physiology. 2023 Jan 13;14:1091248.
45. Yoshinori Aso, Daisuke Hattori, Yang Yu, Rebecca M Johnston, Nirmala A Iyer, Teri-TB Ngo, Heather Dionne, LF Abbott, Richard Axel, Hiromu Tanimoto, Gerald M Rubin (2014) The neuronal architecture of the mushroom body provides a logic for associative learning *eLife* **3**:e04577. https://doi.org/10.7554/eLife.04577
46. Tanaka NK, Tanimoto H, Ito K. Neuronal assemblies of the Drosophila mushroom body. Journal of Comparative Neurology. 2008 Jun 10;508(5):711-55.
47. Mao Z, Davis RL. Eight different types of dopaminergic neurons innervate the Drosophila mushroom body neuropil: anatomical and physiological heterogeneity. Frontiers in neural circuits. 2009 Jul 1;3:612.
48. Hartenstein V, Cruz L, Lovick JK, Guo M. Developmental analysis of the dopamine-containing neurons of the Drosophila brain. Journal of Comparative Neurology. 2017 Feb 1;525(2):363-79.
49. Ueno T, Tomita J, Tanimoto H, Endo K, Ito K, Kume S, Kume K. Identification of a dopamine pathway that regulates sleep and arousal in Drosophila. Nature neuroscience. 2012 Nov;15(11):1516-23.
50. Liu C, Plaçais PY, Yamagata N, Pfeiffer BD, Aso Y, Friedrich AB, Siwanowicz I, Rubin GM, Preat T, Tanimoto H. A subset of dopamine neurons signals reward for odour memory in Drosophila. Nature. 2012 Aug 23;488(7412):512-6.
51. Rohwedder A, Wenz NL, Stehle B, Huser A, Yamagata N, Zlatic M, Truman JW, Tanimoto H, Saumweber T, Gerber B, Thum AS. Four individually identified paired dopamine neurons signal reward in larval Drosophila. Current Biology. 2016 Mar 7;26(5):661-9.
52. Meola G, Cardani R. Myotonic dystrophies: an update on clinical aspects, genetic, pathology, and molecular pathomechanisms. Biochimica et Biophysica Acta (BBA)-Molecular Basis of Disease. 2015 Apr 1;1852(4):594-606.
53. Okkersen K. Brain imaging in myotonic dystrophy type.
54. Huguet A, Medja F, Nicole A, Vignaud A, Guiraud-Dogan C, Ferry A, Decostre V, Hogrel JY, Metzger F, Hoeflich A, Baraibar M. Molecular, physiological, and motor

performance defects in DMSXL mice carrying> 1,000 CTG repeats from the human DM1 locus. PLoS Genetics. 2012 Nov 29;8(11):e1003043.

55. Winblad S, Samuelsson L, Lindberg C, Meola G. Cognition in myotonic dystrophy type 1: a 5-year follow-up study. European journal of neurology. 2016 Sep;23(9):1471-6.
56. Winblad S, Eliasdottir O, Nordström S, Lindberg C. Neurocognitive disorder in Myotonic dystrophy type 1. Heliyon. 2024 May 30;10(10).
57. Okkersen K, Buskes M, Groenewoud J, Kessels RP, Knoop H, van Engelen B, Raaphorst J. The cognitive profile of myotonic dystrophy type 1: a systematic review and meta-analysis. Cortex. 2017 Oct 1;95:143-55.
58. Tschida K, Bhandawat V. Activity in descending dopaminergic neurons represents but is not required for leg movements in the fruit fly D rosophila. Physiological reports. 2015 Mar;3(3):e12322.
59. Johnson N, Hung M, Sansone V, Subramony S, Statland J, Hamel J, van Engelen B, Mul K, Elsheikh B, Roxburgh R, Day J. 463P Longitudinal progression of motor function in individuals with myotonic dystrophy type 1: insights from the END-DM1 study. Neuromuscular Disorders. 2024 Oct 1;43:104441-538.
60. Filli L, Schwegler S, Meyer C, Killeen T, Easthope CS, Broicher SD, Curt A, Zörner B, Bolliger M, Jung HH, Petersen JA. Characterizing cognitive-motor impairments in patients with myotonic dystrophy type 1. Neuromuscular Disorders. 2020 Jun 1;30(6):510-20.
61. Bertrand JA, Jean S, Laberge L, Gagnon C, Mathieu J, Gagnon JF, Richer L. Psychological characteristics of patients with myotonic dystrophy type 1. Acta Neurologica Scandinavica. 2015 Jul;132(1):49-58.
62. Castellano-Guerrero AM, Guerrero R, Relimpio F, Losada F, Mangas MA, Pumar A, Martínez-Brocca MA. Prevalence and predictors of depression and anxiety in adult patients with type 1 diabetes in tertiary care setting. Acta diabetologica. 2018 Sep;55:943-53.
63. Beffy P, Del Carratore R, Masini M, Furling D, Puymirat J, Masiello P, Simili M. Altered signal transduction pathways and induction of autophagy in human myotonic dystrophy type 1 myoblasts. The international journal of biochemistry & cell biology. 2010 Dec 1;42(12):1973-83.
64. Bargiela A, Cerro-Herreros E, Fernandez-Costa JM, Vilchez JJ, Llamusi B, Artero R. Increased autophagy and apoptosis contribute to muscle atrophy in a myotonic dystrophy type 1 Drosophila model. Disease models & mechanisms. 2015 Jul 1;8(7):679-90.

65. Song KY, Guo XM, Wang HQ, Zhang L, Huang SY, Huo YC, Zhang G, Feng JZ, Zhang RR, Ma Y, Hu QZ. MBNL1 reverses the proliferation defect of skeletal muscle satellite cells in myotonic dystrophy type 1 by inhibiting autophagy via the mTOR pathway. Cell Death & Disease. 2020 Jul 18;11(7):545.
66. Bar-Yosef T, Damri O, Agam G. Dual role of autophagy in diseases of the central nervous system. Frontiers in cellular neuroscience. 2019 May 28;13:196.
67. Liu J, Guo ZN, Yan XL, Yang Y, Huang S. Brain pathogenesis and potential therapeutic strategies in myotonic dystrophy type 1. Frontiers in aging neuroscience. 2021 Nov 15;13:755392.